bioRxiv preprint doi: https://doi.org/10.1101/2022.10.24.513634; this version posted October 25, 2022. The copyright holder for this preprint (which was not certified by peer review) is the author/funder, who has granted bioRxiv a license to display the preprint in perpetuity. It is made available under aCC-BY-NC-ND 4.0 International license.

Neuroinvasive flavivirus pathogenesis is restricted by host genetic factors in Collaborative Cross mice, independently of Oas1b

Brittany A. Jasperse[a,*], Melissa D. Mattocks[a,*], Kelsey M. Noll[a,c], Martin T. Ferris[b], Mark T. Heise[a,b], Helen M. Lazear[a]#

[a]Department of Microbiology & Immunology, University of North Carolina at Chapel Hill, Chapel Hill, NC, USA

[b]Department of Genetics, University of North Carolina at Chapel Hill, Chapel Hill, NC, USA

[c]Present address: EpiCypher, Research Triangle Park, NC, USA

*Equal contribution

#Corresponding author

Word count

Abstract: 246

Text: 10,656

bioRxiv preprint doi: https://doi.org/10.1101/2022.10.24.513634; this version posted October 25, 2022. The copyright holder for this preprint (which was not certified by peer review) is the author/funder, who has granted bioRxiv a license to display the preprint in perpetuity. It is made available under aCC-BY-NC-ND 4.0 International license.

ABSTRACT

Powassan virus (POWV) is an emerging tick-borne flavivirus that causes neuroinvasive disease, including encephalitis, meningitis, and paralysis. Similar to other neuroinvasive flaviviruses, such as West Nile virus (WNV) and Japanese encephalitis virus (JEV), POWV disease presentation is heterogeneous, and the factors influencing disease outcome are not fully understood. We used Collaborative Cross (CC) mice to assess the impact of host genetic factors on POWV pathogenesis. We infected a panel of *Oas1b*-null CC lines with POWV and observed a range of susceptibility phenotypes, indicating that host factors other than the well-characterized flavivirus restriction factor *Oas1b* modulate POWV pathogenesis in CC mice. Among *Oas1b*-null CC lines, we identified multiple highly susceptible lines (0% survival), including CC071, and a single resistant line (78% survival), CC045. Susceptibility phenotypes generally were concordant among neuroinvasive flaviviruses, although we identified one line, CC006, that was resistant specifically to JEV, suggesting that both pan-flavivirus and virus-specific mechanisms contribute to susceptibility phenotypes in CC mice. We found that POWV replicated to higher titers in bone marrow-derived macrophages from CC071 mice compared to CC045 mice, suggesting that resistance could result from cell-intrinsic restriction of viral replication. Although serum viral loads at 2 days post-infection were equivalent between CC071 and CC045 mice, clearance of POWV from the serum was significantly slower in CC071 mice. Furthermore, CC045 mice had significantly lower viral loads in the brain at 7 days post-infection compared to CC071 mice, suggesting that reduced CNS infection contributes to the resistant phenotype of CC045 mice.

bioRxiv preprint doi: https://doi.org/10.1101/2022.10.24.513634; this version posted October 25, 2022. The copyright holder for this preprint (which was not certified by peer review) is the author/funder, who has granted bioRxiv a license to display the preprint in perpetuity. It is made available under aCC-BY-NC-ND 4.0 International license.

IMPORTANCE

Neuroinvasive flaviviruses, such as WNV, JEV, and POWV, are transmitted to humans by mosquitoes or ticks, can cause neurologic disease, such as encephalitis, meningitis, and paralysis, and can result in death or long-term sequelae. Although potentially severe, neuroinvasive disease is a rare outcome of flavivirus infection. The factors that determine whether someone develops severe disease after flavivirus infection are not fully understood, but host genetic differences in polymorphic antiviral response genes likely contribute to disease outcome. We evaluated a panel of genetically diverse mice and identified lines with distinct outcomes following infection with POWV. We found that resistance to POWV pathogenesis corresponded to reduced viral replication in macrophages, more rapid clearance of virus in peripheral tissues, and reduced viral infection in the brain. These susceptible and resistant mouse lines will provide a system for investigating the pathogenic mechanisms of POWV and identifying polymorphic host genes that contribute to resistance.

bioRxiv preprint doi: https://doi.org/10.1101/2022.10.24.513634; this version posted October 25, 2022. The copyright holder for this preprint (which was not certified by peer review) is the author/funder, who has granted bioRxiv a license to display the preprint in perpetuity. It is made available under aCC-BY-NC-ND 4.0 International license.

INTRODUCTION

Neuroinvasive flaviviruses such as West Nile virus (WNV), Japanese encephalitis virus (JEV), St. Louis encephalitis virus (SLEV), tick-borne encephalitis virus (TBEV), and Powassan virus (POWV) are transmitted to humans by mosquitoes or ticks and can spread from the circulation into the central nervous system (CNS) (1, 2). Flavivirus infections exhibit a heterogenous presentation, with ~80% of infections being asymptomatic and ~20% presenting with febrile symptoms. A subset of individuals with symptomatic WNV, JEV, SLEV, TBEV, or POWV infection progress to severe, neuroinvasive disease (e.g., encephalitis, meningitis, or paralysis), which can be fatal or lead to long-term cognitive and functional sequelae. Neurologic disease can result from direct viral infection of neurons and also from the inflammatory response triggered by a viral infection of the CNS. However, the factors influencing susceptibility to severe neuroinvasive disease remain incompletely understood.

POWV is an emerging tick-borne flavivirus within the tick-borne encephalitis serocomplex that is transmitted by the same *Ixodes* ticks that transmit Lyme disease (3). POWV is the only tick-borne flavivirus found in North America. Like other tick-borne diseases, the incidence of POWV infection is increasing (4). POWV was first isolated from the brain of a young boy who died of encephalitis in 1958 in Powassan, Ontario, Canada (5). Forty years later, a virus sharing 94% amino acid identity with POWV was isolated from a deer tick (*Ixodes scapularis*), and was named deer tick virus (DTV) (6, 7). POWV circulates as two distinct but serologically indistinguishable genotypes: Lineage I containing the prototype POWV, and Lineage II, containing DTV (6-8). Infection with POWV can have devastating impacts, as approximately 10% of reported encephalitic

bioRxiv preprint doi: https://doi.org/10.1101/2022.10.24.513634; this version posted October 25, 2022. The copyright holder for this preprint (which was not certified by peer review) is the author/funder, who has granted bioRxiv a license to display the preprint in perpetuity. It is made available under aCC-BY-NC-ND 4.0 International license.

cases of POWV are fatal, and over 50% of survivors experience long-term cognitive and functional sequelae (9).

Flavivirus infection in humans is characterized by significant variation in disease severity, suggesting that host genetic factors impact the probability and outcome of neuroinvasive disease (10-16). Host genes related to the antiviral immune response have been associated with the outcome of flavivirus infection in humans (16). For example, polymorphisms in the dsRNA sensor OAS1 and the chemokine receptor CCR5 are associated with WNV and TBEV infection, symptomatic presentation, and neuroinvasive disease (10, 14, 17, 18). Flavivirus resistance is one of the earliest examples of a genetic determinant of pathogen susceptibility defined in mice. In the 1930s, resistance to flavivirus disease was shown to be inherited in mice (19) and in the 2000s, resistance was mapped to the 2′-5′ oligoadenylate synthetase 1b (*Oas1b*) gene (20, 21). The antiviral activity of Oas1b restricts all flaviviruses tested and appears to act exclusively against flaviviruses. Genetic resistance to tick-borne flavivirus disease was demonstrated in the 1930s by selective breeding of mouse lines that were either resistant or susceptible to TBEV and louping ill virus (22, 23) and similar studies demonstrated differential susceptibility to the mosquito-borne flaviviruses St. Louis encephalitis virus and yellow fever virus (24-28).

The Collaborative Cross (CC) is a mouse genetic reference population of recombinant inbred lines. These lines were generated by crossing eight founder strains that represent three wild-derived and five classical laboratory mouse lines and then independently inbreeding each family deriving from one of these 8-founder funnels (29, 30). The CC captures the genetic diversity of laboratory mice, roughly on par with levels

bioRxiv preprint doi: https://doi.org/10.1101/2022.10.24.513634; this version posted October 25, 2022. The copyright holder for this preprint (which was not certified by peer review) is the author/funder, who has granted bioRxiv a license to display the preprint in perpetuity. It is made available under aCC-BY-NC-ND 4.0 International license.

of common human genetic variation, in a reproducible manner, since each of the 63 lines has a known and fixed genome, providing a valuable tool for mapping complex traits (29-33). As such, the CC enables the identification and study of polymorphic host genes underlying complex phenotypes including the immune response to viral infection (29-35). Further, since each line is inbred, the CC can be used to facilitate the study of phenotypes that are diverse and dynamic through time (such as the response to infection) in a reproducible manner.

Common laboratory mouse lines (including CC founder lines C57BL/6, A/J, 129, NOD, and NZO) have truncated *Oas1b* alleles that lack 30% of the C terminal sequence due to a premature stop codon, whereas wild-derived lines (CC founder lines WSB, PWK, and CAST) each have unique full-length *Oas1b* alleles, meaning that CC lines carry either a full-length or truncated allele of *Oas1b*. Previous studies using F1 hybrids of CC mice to define genetic determinants of WNV pathogenesis found via genetic mapping that *Oas1b* had a major impact on WNV disease outcome (36, 37). However, the mechanism by which Oas1b restricts flavivirus infection remains unclear, since both full-length and truncated Oas1b proteins lack synthetase activity (38, 39), although full-length Oas1b does inhibit Oas1a synthetase activity and reduces 2′-5′ linked oligoadenylate production (38).

In this study, we used CC mice to investigate the effect of host genetics on disease outcome following neuroinvasive flavivirus infection. We found that a panel of *Oas1b*^{null} CC lines had a range of susceptibility phenotypes following POWV infection and we used susceptible and resistant lines to investigate mechanisms of POWV pathogenesis. We found that resistance to POWV pathogenesis corresponded to reduced viral replication in

bioRxiv preprint doi: https://doi.org/10.1101/2022.10.24.513634; this version posted October 25, 2022. The copyright holder for this preprint (which was not certified by peer review) is the author/funder, who has granted bioRxiv a license to display the preprint in perpetuity. It is made available under aCC-BY-NC-ND 4.0 International license.

129 macrophages, more rapid clearance of virus in peripheral tissues, and reduced viral
130 infection in the brain. These findings reveal diverse pathologic outcomes of POWV
131 infection in CC mice and suggest that rapid clearance of POWV in the periphery
132 contributes to reduced neuroinvasion and resistance to lethality. These susceptible and
133 resistant mouse lines will provide a system for investigating the pathogenic mechanisms
134 of POWV and identifying polymorphic host genes that contribute to resistance.
135
136 **RESULTS**
137
138 ***Oas1b* restricts pathogenesis of neuroinvasive flaviviruses.** To assess the effect of
139 *Oas1b* on neuroinvasive flavivirus pathogenesis in CC mice, we infected three strains of
140 mice: wild-type C57BL/6J (non-functional *Oas1b* allele); CC019 (functional *Oas1b* allele
141 derived from the WSB founder strain), and an *Oas1b*^{del} line on a CC019 background
142 generated by CRISPR/Cas-9 gene editing (see Methods). We infected 5-6-week-old mice
143 with 100 FFU of POWV (strains LB or DTV Spooner), WNV, or JEV and monitored
144 survival for 21 days (Fig. 1A-D). As expected, CC019 mice were resistant to all three
145 viruses, consistent with a strong effect of *Oas1b* on susceptibility to neuroinvasive
146 flaviviruses. We found that CC019-*Oas1b*^{del} mice were susceptible to POWV LB, POWV
147 DTV, WNV, and JEV (80%, 73%, 75% and 60% lethality, respectively). To determine
148 whether genetic determinants of susceptibility in mice corresponded to differences in viral
149 replication, we performed multi-step growth curves in primary mouse embryo fibroblasts
150 (MEFs). We generated MEFs from C57BL/6J, CC019, and CC019-*Oas1b*^{del} mice,
151 infected with POWV or WNV at an MOI of 0.1, and measured viral titers in the culture

bioRxiv preprint doi: https://doi.org/10.1101/2022.10.24.513634; this version posted October 25, 2022. The copyright holder for this preprint (which was not certified by peer review) is the author/funder, who has granted bioRxiv a license to display the preprint in perpetuity. It is made available under aCC-BY-NC-ND 4.0 International license.

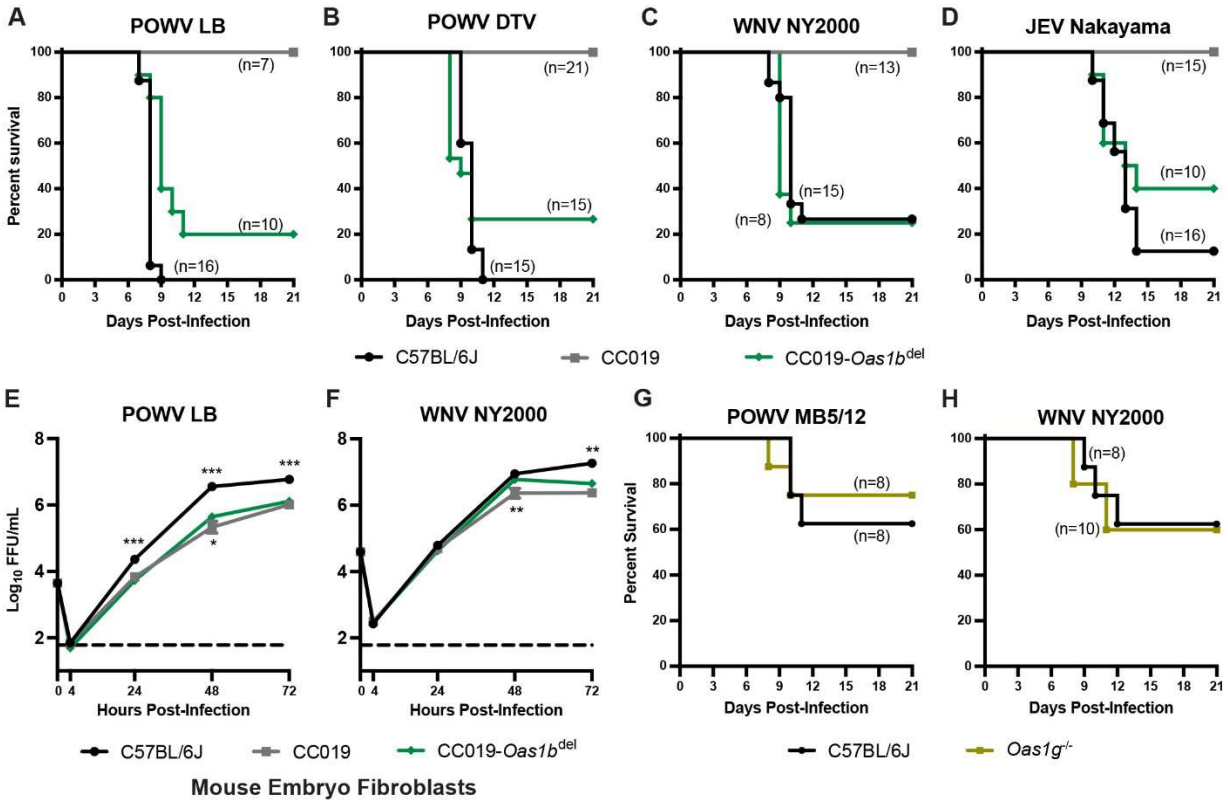

Figure 1. Oas1b restricts pathogenesis of diverse neuroinvasive flaviviruses. A-D. Five to six-week-old male and female CC019, CC019-*Oas1b*^{del}, or C57BL/6J mice were infected with 100 FFU of POWV strain LB (A), POWV DTV strain Spooner (B), WNV strain NY2000 (C), or JEV strain Nakayama (D) by subcutaneous inoculation in the footpad and lethality was monitored for 21 days. Data are combined from 4-5 experiments per virus. E-F. Mouse embryo fibroblasts (MEFs) were harvested from the indicated mouse lines for multistep growth curve analysis. MEFs were infected at an MOI of 0.01 with POWV strain LB (E) or WNV strain NY2000 (F). Supernatants were collected at 4, 24, 48, or 72 hours post-infection and titered by focus-forming assay on Vero cells. Results shown are the mean +/- SEM of 2-3 independent experiments performed in duplicate or triplicate. Asterisks represent statistical significance (* p<0.05, ** p<0.01, *** p<0.001) by two-way ANOVA compared to CC019-*Oas1b*^{del}. G-H. Nine to twelve-week-old C57BL/6J wild-type or *Oas1g*$^{-/-}$ male and female mice were infected with 100 FFU of POWV strain MB5/12 (G) or WNV strain NY2000 (H) by subcutaneous inoculation in the footpad and lethality was monitored for 21 days.

supernatant over 72 hrs (Fig. 1E-F). POWV replication was significantly higher in MEFs derived from C57BL/6J mice compared to CC019-*Oas1b*^{del} mice starting at 24 hpi (Fig. 1E), with a maximum difference of 8-fold at 48 hpi; WNV-infected MEFs were only significantly different at 72 hpi (4-fold) (Fig. 1F). POWV and WNV replication in CC019-*Oas1b*^{del} MEFs were only modestly increased compared to CC019 MEFs (2- and 3-fold, respectively), and only at 48 hpi. Altogether these results suggest that non-Oas1b genetic factors are responsible for the differences in viral replication in MEFs.

bioRxiv preprint doi: https://doi.org/10.1101/2022.10.24.513634; this version posted October 25, 2022. The copyright holder for this preprint (which was not certified by peer review) is the author/funder, who has granted bioRxiv a license to display the preprint in perpetuity. It is made available under aCC-BY-NC-ND 4.0 International license.

Humans have four paralogous OAS genes: *OAS1*, *OAS2*, *OAS3*, and *OASL*. Mice, however, have single copies of *Oas2* and *Oas3*, two copies of *OasL*, and eight copies of *Oas1* (*Oas1a*-*Oas1h*) (39). To determine whether other *Oas1* paralogs play a similar role in restricting flavivirus pathogenesis as *Oas1b*, we infected 9 to 12-week-old *Oas1g*$^{-/-}$ mice (C57BL/6N background) or wild-type mice (C57BL/6J background) with POWV strain MB5/12 or WNV and monitored lethality for 21 days. These older mice were more resistant to POWV and WNV pathogenesis compared to the 5- to 6-week-old mice used in the previous experiments, but we found no significant difference in survival for *Oas1g*$^{-/-}$ mice compared to wild-type (Fig. 1G-H), suggesting the function of *Oas1b* as a flavivirus restriction factor is not conserved among all *Oas1* paralogs.

***Oas1b*-null Collaborative Cross lines exhibit a range of susceptibility phenotypes to neuroinvasive flaviviruses.** To investigate the role of host genetic factors outside of the well-known flavivirus restriction factor *Oas1b*, we infected mice from a panel of 16 CC strains (9 to 12-week-old mice, all lines possessing *Oas1b*^{null} alleles), as well as CC019-*Oas1b*^{del} mice, with POWV strain LB and monitored lethality for 21 days (Fig. 2 and Table 1). As expected, most lines were highly susceptible to POWV (100% lethality in 11 of 17 CC lines). However, we identified one

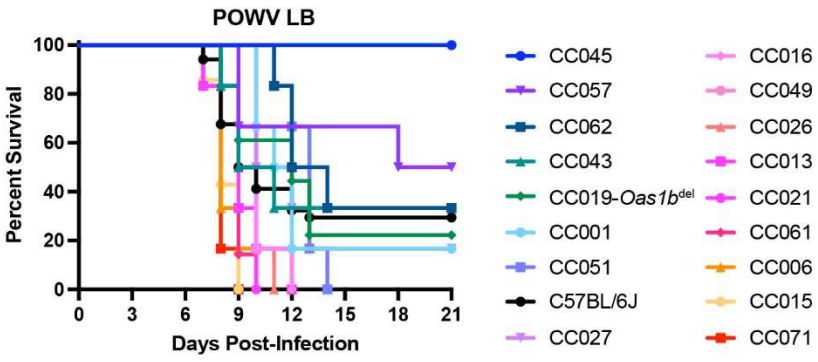

Figure 2. Host factors influence POWV pathogenesis across *Oas1b*-null Collaborative Cross mouse lines. Nine to twelve-week-old male and female mice were infected with 100 FFU of POWV (strain LB) by subcutaneous inoculation in the footpad and lethality was monitored for 21 days. Lines are ordered by percent survival and mean time to death. N=34 C67BL/6 mice, 18 CC019-*Oas1b*^{del} mice, and 6-7 mice for other lines. Data are combined from 9 experiments.

bioRxiv preprint doi: https://doi.org/10.1101/2022.10.24.513634; this version posted October 25, 2022. The copyright holder for this preprint (which was not certified by peer review) is the author/funder, who has granted bioRxiv a license to display the preprint in perpetuity. It is made available under aCC-BY-NC-ND 4.0 International license.

resistant line (CC045, 0% lethality), and five lines with intermediate susceptibility (CC001, CC027, CC043, CC057, CC062, 50-83% lethality).

To validate the phenotypes observed with POWV strain LB, we infected a subset of the Oas1b^{null} CC lines with POWV strain MB5/12, WNV strain NY2000, JEV strain Nakayama, or St. Louis encephalitis virus (SLEV) strain GHA-3 and monitored lethality for 21 days (Fig. 3A-D). CC071 mice were highly susceptible to all viruses tested, with 100% lethality observed after infection with POWV MB5/12 (Fig. 3A) or WNV (Fig. 3B), 91% lethality in JEV-infected mice (Fig. 3C). CC071 mice exhibited 57% lethality after SLEV infection, which was remarkable as C57BL/6J and CC019-*Oas1b*^{del} mice exhibited no lethality after SLEV infection (Fig. 3D). Furthermore, CC045 mice, which were the most resistant CC line to POWV LB (100% survival, Fig. 2), also were relatively resistant to POWV MB5/12 (78% survival, Fig. 3A), WNV (50% survival, Fig. 3B), and JEV (50%

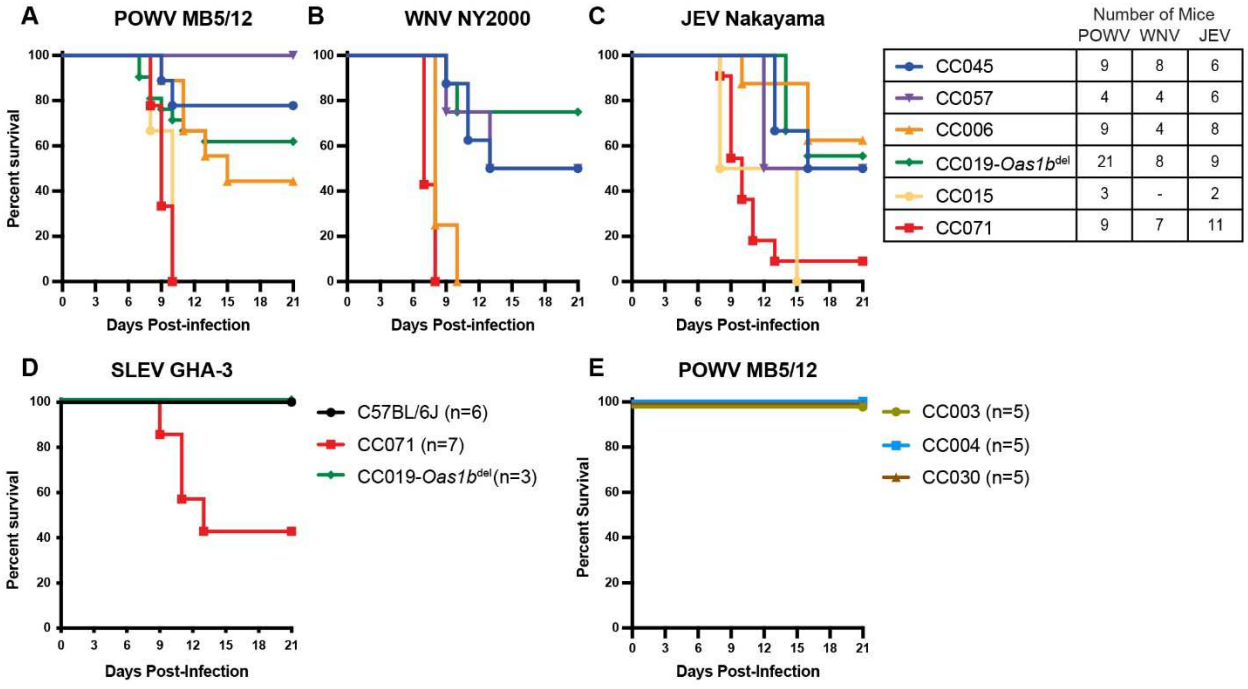

Figure 3. Susceptibility phenotypes in Collaborative Cross mice are shared among diverse neuroinvasive flaviviruses. A-D. Nine to twelve-week-old male and female mice from Oas1b-null CC lines were infected with 100 FFU of POWV strain MB5/12 (A), WNV strain NY2000 (B), JEV strain Nakayama (C), or SLEV strain GHA-3 (D) by subcutaneous inoculation in the footpad and lethality was monitored for 21 days. Data are combined from 4-8 experiments per virus. E. Nine to twelve-week-old male mice from *Oas1b*+/+ CC lines were infected with 100 FFU of POWV strain MB5/12 and lethality was monitored for 21 days. Data represent a single experiment.

bioRxiv preprint doi: https://doi.org/10.1101/2022.10.24.513634; this version posted October 25, 2022. The copyright holder for this preprint (which was not certified by peer review) is the author/funder, who has granted bioRxiv a license to display the preprint in perpetuity. It is made available under aCC-BY-NC-ND 4.0 International license.

194 survival, Fig. 3C). Thus, most susceptibility phenotypes were concordant among POWV,
195 WNV, and JEV. However, some lines exhibited virus-specific susceptibility. CC006 mice
196 were highly susceptible to WNV (100% lethality, Fig. 3B), intermediately susceptible to
197 POWV MB5/12 (56% lethality, Fig. 3A), yet were the most resistant CC line to JEV (37%
198 lethality, Fig. 3C). This suggests that there are both pan-flavivirus and virus-specific
199 mechanisms that control susceptibility to neuroinvasive flaviviruses. We also evaluated
200 CC lines with functional *Oas1b* alleles (CC003, WSB allele; CC004, PWK allele; and
201 CC030, WSB allele). As expected, these mice were resistant to POWV MB5/12 infection
202 (0% lethality, Fig. 3E), further supporting that functional *Oas1b* alleles derived from
203 different CC founder lines restrict neuroinvasive flavivirus pathogenesis in CC mice.
204
205 **Susceptibility of Collaborative Cross lines to neuroinvasive flavivirus**
206 **pathogenesis does not correlate with early viremia levels.** To uncover the pathogenic
207 mechanisms behind the differences in flavivirus susceptibility among *Oas1b*^{null} CC lines,
208 we investigated whether resistance to lethality corresponded with decreased viremia. We
209 measured viral loads in the serum by quantitative reverse transcription-PCR (qRT-PCR)
210 in serum collected 2 dpi from *Oas1b*^{null} CC lines (CC045, CC057, CC006, CC019-*Oas1b*$^{-}$
211 $^{/-}$, CC015, and CC071) infected with POWV, WNV, or JEV (Fig. 4). Surprisingly, we found
212 no concordance between mean viremia (Fig. 4A, C, D) and susceptibility (Fig. 3A-C)
213 among the *Oas1b*^{null} CC lines tested. Furthermore, viral loads in the serum were similar
214 between *Oas1b*^{null} CC mice (Fig. 4A) and *Oas1b*$^{+/+}$ CC mice (Fig. 4B). Moreover, within
215 CC lines, there was no difference in viremia between mice that survived (open symbols)
216 compared to mice that succumbed to infection (closed symbols). These data suggest that

bioRxiv preprint doi: https://doi.org/10.1101/2022.10.24.513634; this version posted October 25, 2022. The copyright holder for this preprint (which was not certified by peer review) is the author/funder, who has granted bioRxiv a license to display the preprint in perpetuity. It is made available under aCC-BY-NC-ND 4.0 International license.

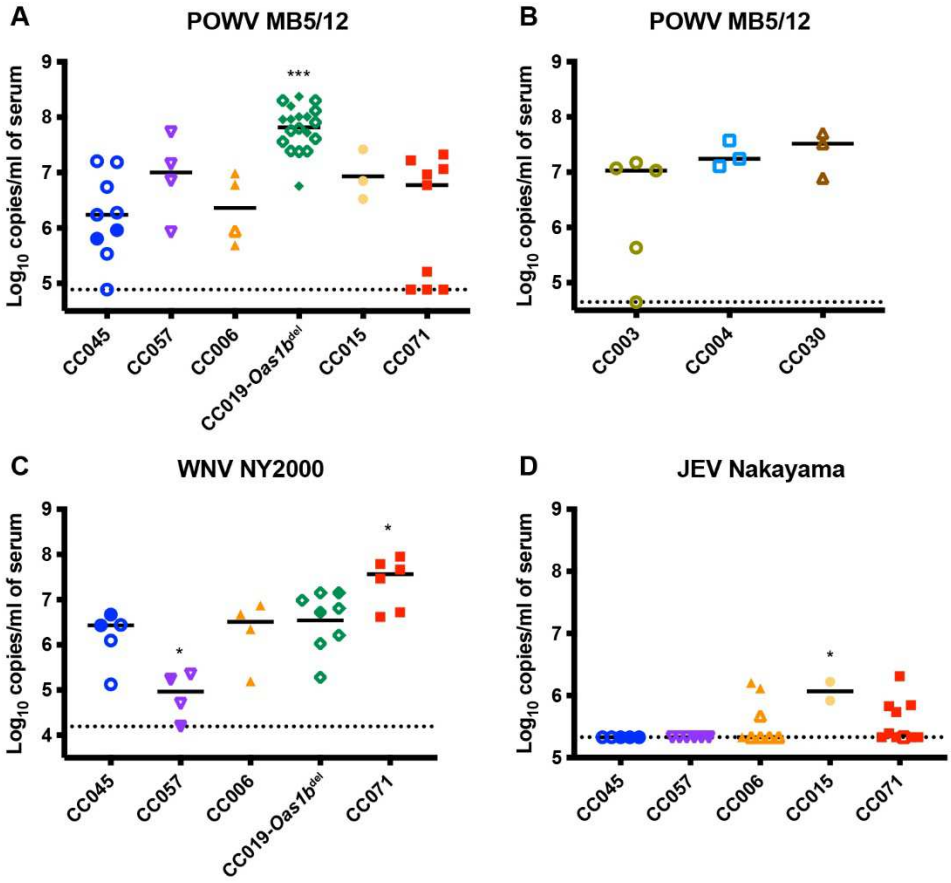

Figure 4. Serum viral loads at 2 dpi do not correlate with susceptibility to neuroinvasive flaviviruses. Nine to twelve-week-old male and female mice were infected with 100 FFU of POWV (A and B), WNV (C), or JEV (D) by subcutaneous inoculation in the footpad. Mice were bled 2 dpi and viremia was assessed by qRT-PCR. Asterisks represent statistical significance (* $p<0.05$, *** $p<0.001$) by one-way ANOVA compared to CC045 (panels A, C, and D). CC lines in A, C, and D are all *Oas1b*-null; CC lines in B are *Oas1b*+/+. Open symbols denote surviving mice.

controlling viremia at 2 dpi is not the mechanism of resistance to flavivirus pathogenesis in these CC lines.

Resistance to neuroinvasive flavivirus pathogenesis correlates with reduced replication in macrophages. To evaluate whether resistance to POWV disease corresponds with cell-intrinsic restriction of viral replication, we generated bone marrow-derived macrophages (BMDM) from CC mice and performed multi-step growth curves with POWV and WNV (Fig. 5). BMDMs from CC071 and CC015 mice produced

bioRxiv preprint doi: https://doi.org/10.1101/2022.10.24.513634; this version posted October 25, 2022. The copyright holder for this preprint (which was not certified by peer review) is the author/funder, who has granted bioRxiv a license to display the preprint in perpetuity. It is made available under aCC-BY-NC-ND 4.0 International license.

significantly higher viral titers of POWV compared to BMDMs from CC045 mice (417-fold and 24-fold higher at 72 hpi) (Fig. 5A),

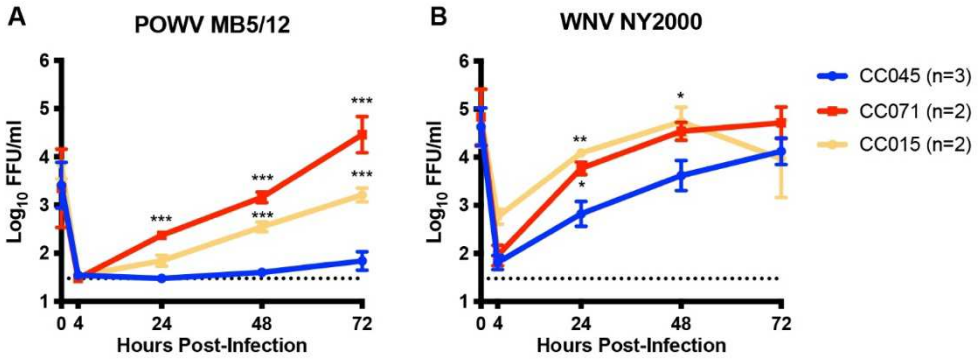

Figure 5. Susceptibility to flavivirus disease is concordant with restriction of viral replication in macrophages ex vivo. Bone marrow-derived macrophages (BMDM) were harvested from CC mice (CC045, CC071, and CC015) for multistep growth curve analysis. BMDMs were infected at an MOI of 0.01 with POWV (A) or WNV (B). Supernatants were collected at 4, 24, 48, or 72 hours post-infection and titered by focus-forming assay on Vero cells. Results shown are the mean +/- SEM of 2-3 independent experiments performed in duplicate or triplicate. Asterisks represent statistical significance (* $p<0.05$, *** $p<0.001$) by two-way ANOVA compared to CC045.

concordant with the increased susceptibility of CC071 and CC015 mice to POWV infection (Fig. 3A). Similarly, BMDMs from CC015 mice exhibited enhanced WNV replication at 24 and 48 hpi, and CC071-derived BMDMs had significantly higher viral titers at 24 hpi, compared to BMDMs from CC045 mice (18-fold and 9-fold higher at 24 hpi) (Fig. 5B). Thus, resistance to flavivirus disease in CC mice could result from cell-intrinsic restriction of viral replication in macrophages, a key cellular target of flaviviruses *in vivo*.

Resistance to POWV pathogenesis correlates with rapid clearance of peripheral infection and lower CNS viral loads. Although we found no difference in serum viral loads at 2 dpi between susceptible and resistant CC lines (Fig. 4), susceptibility to neuroinvasive flaviviruses could be driven by serum viral loads at later time points, or by viral loads in the CNS, independent of viremia. To further investigate the pathogenic mechanisms of POWV infection, we infected CC lines identified as susceptible (CC071)

bioRxiv preprint doi: https://doi.org/10.1101/2022.10.24.513634; this version posted October 25, 2022. The copyright holder for this preprint (which was not certified by peer review) is the author/funder, who has granted bioRxiv a license to display the preprint in perpetuity. It is made available under aCC-BY-NC-ND 4.0 International license.

and resistant (CC045) and measured viral loads in serum, spleen, and brain at 3 and 7 dpi. CC071 mice exhibited high viremia at 3 dpi (mean 7.9 log_{10} copies/ml of serum) and POWV RNA was detected in the serum of all 8 CC071 mice harvested at 7 dpi (Fig. 6A). However, 2 of 5 CC045 mice had cleared POWV from the serum by 3 dpi, and viremia was low in the remaining CC045 mice (maximum 5.7 log_{10} copies/ml of serum), and

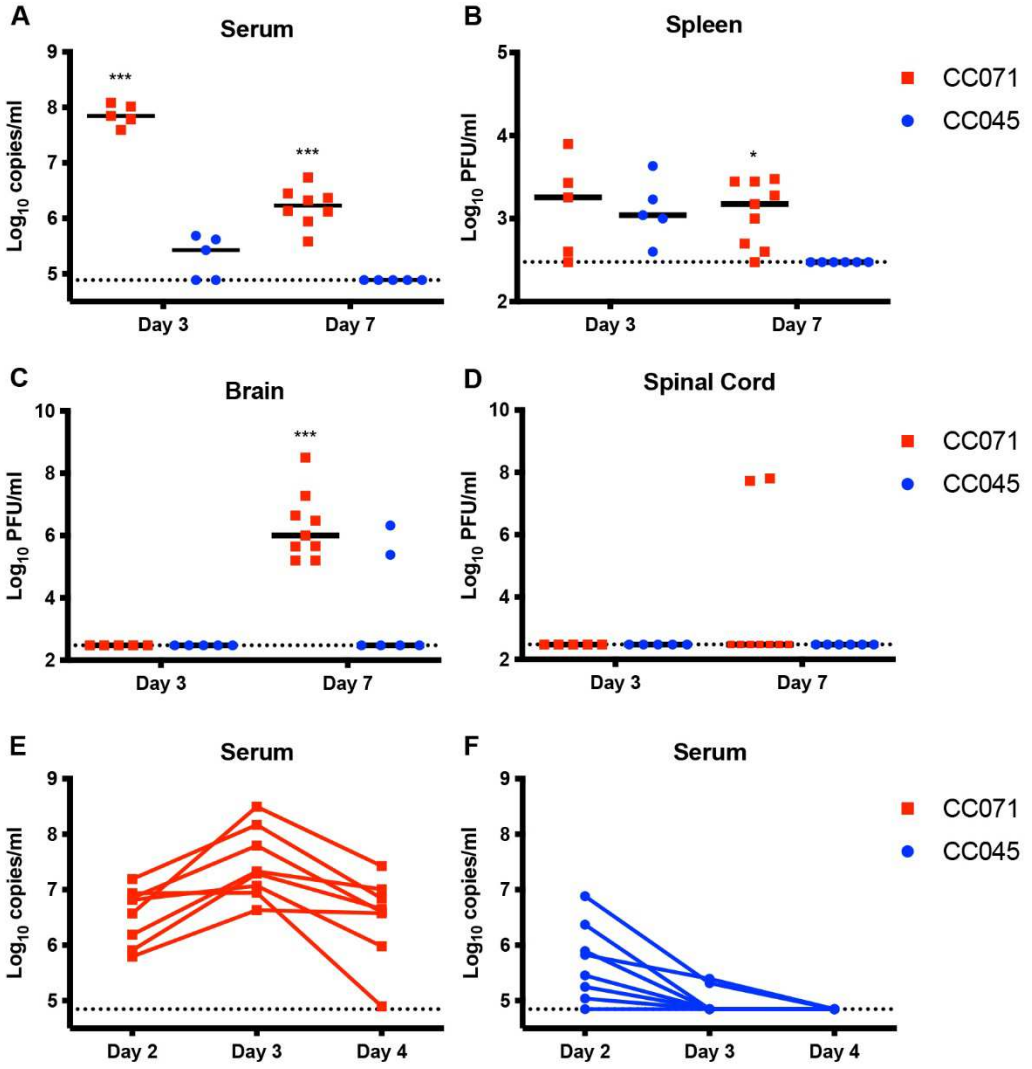

Figure 6. Reduced CNS viral loads correlate with POWV resistance. Nine to twelve-week-old male and female CC071 (susceptible) and CC045 (resistant) mice were infected with 100 FFU of POWV (strain MB5/12) by subcutaneous inoculation in the footpad. A-D. At the indicated time points, mice were perfused and tissues were harvested. A. Mice were bled by cardiac puncture prior to perfusion and viremia was assessed by qRT-PCR. B-D. Spleen, brain, and spinal cord homogenates were titered by plaque assay on Vero cells. E-F. Mice were serially bled 2, 3, and 4 dpi and viremia was assessed by qRT-PCR. Asterisks represent statistical significance (* $p<0.05$, *** $p<0.001$) by two-way ANOVA.

bioRxiv preprint doi: https://doi.org/10.1101/2022.10.24.513634; this version posted October 25, 2022. The copyright holder for this preprint (which was not certified by peer review) is the author/funder, who has granted bioRxiv a license to display the preprint in perpetuity. It is made available under aCC-BY-NC-ND 4.0 International license.

253 POWV RNA was not detected in the serum of any of the 5 CC045 mice harvested at 7
254 dpi (Fig. 6A). This suggests that while viral loads in the serum at 2 dpi were equivalent
255 between susceptible (CC071) and resistant (CC045) lines (Fig. 4A), clearance of POWV
256 from the serum was faster in CC045 mice. Despite a >350-fold difference in serum viral
257 loads at 3 dpi between CC071 and CC045 mice, we found no significant difference in
258 spleen viral loads at 3 dpi (Fig. 6B). In contrast, by 7 dpi, all CC045 mice had cleared
259 POWV from the spleen, while CC071 mice had viral loads in the spleen similar to those
260 observed at 3 dpi (Fig. 6B), concordant with the sustained viremia in CC071 mice through
261 7 dpi (Fig. 6A). We also assessed viral loads in the CNS and found that POWV was
262 undetectable in the brains of CC071 and CC045 mice at 3 dpi, but by 7 dpi, all CC071
263 mice had high viral loads in the brain (mean 6.3 Log_{10} PFU/ml) (Fig. 6C). Interestingly,
264 while 4 of 6 CC045 mice had undetectable viral loads in the brain at 7 dpi, the remaining
265 2 mice had brain viral loads similar to CC071 mice (maximum 6.3 log_{10} PFU/ml) (Fig. 6C).
266 The observation that 33% of CC045 mice had detectable virus in the brain at 7 dpi (Fig.
267 6C) is concordant with our earlier observation that CC045 mice had 22% lethality to
268 POWV strain MB5/12 (Fig. 3A). POWV was undetectable in the spinal cords of CC071
269 mice at 3 dpi, but by 7 dpi, 2 of 9 CC071 mice had high viral loads in the spinal cord
270 (maximum 7.8 log_{10} PFU/ml) (Fig. 6D). Interestingly, the 2 CC071 mice that had high viral
271 loads in the spinal cord also had the highest viral loads in the brain at 7 dpi, suggesting
272 the presence of POWV in the spinal cord is due to viral spread within the CNS rather than
273 separate stochastic breaches of the blood-brain barrier (BBB). Further, POWV was not
274 detected in spinal cords from CC045 mice at 3 or 7 dpi (Fig. 6D). Altogether, these data

bioRxiv preprint doi: https://doi.org/10.1101/2022.10.24.513634; this version posted October 25, 2022. The copyright holder for this preprint (which was not certified by peer review) is the author/funder, who has granted bioRxiv a license to display the preprint in perpetuity. It is made available under aCC-BY-NC-ND 4.0 International license.

suggest the mechanism of resistance to POWV infection in CC045 mice is the prevention of neuroinvasion.

To further investigate differences in the rate of clearance of POWV from the periphery in susceptible and resistant mice, we infected CC071 and CC045 mice and performed serial measurements of viral loads in the serum at 2, 3, and 4 dpi to analyze the kinetics of viremia in individual mice. Consistent with our previous experiments, we found that CC071 mice had high viral loads at 2 dpi (mean 6.5 log_{10} copies/ml), which peaked at 3 dpi (mean 7.5 log_{10} copies/ml), and remained high in 7 of 8 mice at 4 dpi (mean 6.5 log_{10} copies/ml) (Fig. 6D). While CC045 mice had high viral loads in the serum at 2 dpi (mean 5.7 Log_{10} copies/ml), 6 of 8 mice had undetectable viremia at 3 dpi, and all mice had cleared by 4 dpi (Fig. 6E). The viremia kinetics observed in individual CC045 and CC071 mice (Fig. 6D-E) are concordant with our earlier observation in terminally-bled mice that CC045 mice clear POWV from the periphery more rapidly than CC071 mice (Fig. 6A). Altogether, these data support a model of POWV pathogenesis in which rapid clearance of viremia reduces the likelihood of virus breaching the BBB and accessing the CNS, where viral infection results in mortality.

DISCUSSION

In this study, we investigated the effect of host genetics on disease outcome following neuroinvasive flavivirus infection. We found that a panel of *Oas1b*^{null} CC lines had a range of susceptibility phenotypes following POWV infection, indicating that polymorphic host genes other than *Oas1b* contribute to disease outcome after POWV infection. We identified *Oas1b*^{null} CC lines that are susceptible (100% lethality) or resistant

bioRxiv preprint doi: https://doi.org/10.1101/2022.10.24.513634; this version posted October 25, 2022. The copyright holder for this preprint (which was not certified by peer review) is the author/funder, who has granted bioRxiv a license to display the preprint in perpetuity. It is made available under aCC-BY-NC-ND 4.0 International license.

(<25% lethality) to POWV and used these lines to investigate mechanisms of POWV pathogenesis. We observed reduced POWV and WNV replication in primary macrophages derived from resistant mice, suggesting resistance to flavivirus disease in CC mice could result from cell-intrinsic restriction of viral replication in macrophages. We found no differences in POWV viremia between susceptible and resistant CC mice at 2 dpi but found that resistant mice cleared POWV from the periphery rapidly whereas susceptible mice had high viremia throughout the infection. Further, we observed significant differences in viral loads in the brains of susceptible and resistant CC mice following POWV infection. These findings reveal diverse pathologic outcomes of POWV infection in CC mice and suggest that rapid clearance of POWV in the periphery contributes to reduced neuroinvasion and protection from lethality.

Neuroinvasive flaviviruses, such as WNV, JEV, and POWV, can cause neurologic disease, such as encephalitis, meningitis, and paralysis, and can result in death or long-term cognitive and functional sequelae (1, 2, 40). JEV is the most prevalent cause of viral encephalitis worldwide, causing an estimated 68,000 cases and >10,000 deaths annually throughout east and southeast Asia, even though a vaccine is available (41, 42). In 2022, local transmission of JEV was detected in Australia for the first time since 1995 and ultimately led to dozens of reported JEV cases within Australia (43). In North America, West Nile virus (WNV) is the most common cause of viral encephalitis, with 1,855 cases of West Nile neuroinvasive disease reported to the CDC in 2021 and a total of 25,849 US cases since 1999 when the virus was introduced to North America (44). While JEV and WNV are transmitted to humans by mosquitoes, TBEV and POWV are transmitted by ticks. TBEV causes >10,000 cases of encephalitis annually in Europe and Asia despite

bioRxiv preprint doi: https://doi.org/10.1101/2022.10.24.513634; this version posted October 25, 2022. The copyright holder for this preprint (which was not certified by peer review) is the author/funder, who has granted bioRxiv a license to display the preprint in perpetuity. It is made available under aCC-BY-NC-ND 4.0 International license.

the availability of a vaccine (45, 46). POWV is the only tick-borne flavivirus found in North America and like other tick-borne diseases, the incidence of POWV infection is increasing (4). Given the clinical importance of endemic neuroinvasive flaviviruses, as well as the potential for related flaviviruses such as Usutu virus (USUV) to emerge as new human pathogens (47, 48), it is important to understand the factors that lead to severe clinical outcomes after infection with these viruses.

Neurotropic viruses, including neuroinvasive flaviviruses, can cause disease by direct damage to infected neurons, as well as by stimulating pathogenic inflammatory responses (49-52). The pathogenic mechanisms of neuroinvasive flaviviruses have been studied extensively in mice, which recapitulate key features of human disease such as neuronal infection, immune infiltration into the CNS, paralysis, encephalitis, and cognitive loss. Much of this work has focused on WNV, but more recent studies have investigated POWV pathogenesis in mice; these studies have studied POWV disease using laboratory mouse lines such as C57BL/6J and Balb/c, as well as *Peromyscus* mice which are thought to serve as reservoirs for Lineage II POWV (DTV) in nature (53-57). C57BL/6J mice are highly susceptible to POWV, which makes them useful for modeling severe human disease, but makes them less useful for defining the mechanisms that allow the majority of infected individuals to sustain mild or asymptomatic infections while a small subset of infected individuals develop severe neuroinvasive disease. Comparing POWV infection in resistant CC lines (e.g., CC045) to susceptible lines (e.g., CC071) has the potential to reveal which aspects of POWV infection and the resulting host immune response (e.g., viral loads in the periphery, persistent viremia, neuroinvasion, replication within the CNS, damage to CNS neurons, neuroinflammation, etc.) correlate with severe

bioRxiv preprint doi: https://doi.org/10.1101/2022.10.24.513634; this version posted October 25, 2022. The copyright holder for this preprint (which was not certified by peer review) is the author/funder, who has granted bioRxiv a license to display the preprint in perpetuity. It is made available under aCC-BY-NC-ND 4.0 International license.

neurologic disease. CC mice can be useful models of relevant disease presentations that are not evident in conventional laboratory mouse lines, such as encephalitis caused by Rift Valley fever virus (34) or chronic WNV disease (58).

Altogether, our results support a model in which CC045 mice are resistant to severe POWV disease due to reduced viral replication in myeloid cells and rapid clearance of viremia, reducing the probability of neuroinvasion, and that this resistance is independent of a role for Oas1b in restricting flavivirus pathogenesis. This model suggests that the resistance mechanism of CC045 mice acts in peripheral tissues, not within the CNS. Although the mechanisms by which flaviviruses cross the blood-brain barrier and invade the CNS remain incompletely understood (59), hematogenous neuroinvasion likely is somewhat stochastic and prolonged high viremia (e.g., in CC071 mice) increases the probability of virus crossing the BBB. We expect that once any POWV accesses the CNS it encounters a highly permissive and sensitive environment, resulting in uniform lethality. Accordingly, while we detected no virus in the brains of most CC045 mice, 2 of 6 CC045 mice did have virus in their brains and at levels equivalent to CC071 mice, consistent with the ~22% lethality we observed for CC045 mice. The model that CC045 resistance results from rapid clearance of viremia is somewhat at odds with the observation that susceptibility did not correlate with 2 dpi viremia either within or among CC lines. However, this model is supported by the distinct viremia kinetics between CC045 and CC071 mice and suggests that rapid clearance, but not peak viremia, is a key determinant of POWV susceptibility in CC mice. Future studies will characterize viral replication in cell types other than macrophages and will compare CNS immune infiltrates

bioRxiv preprint doi: https://doi.org/10.1101/2022.10.24.513634; this version posted October 25, 2022. The copyright holder for this preprint (which was not certified by peer review) is the author/funder, who has granted bioRxiv a license to display the preprint in perpetuity. It is made available under aCC-BY-NC-ND 4.0 International license.

and CNS pathology in CC045 mice versus CC071 to determine whether these lines differ in BBB permeability at baseline and in response to POWV infection.

In general, the susceptibility phenotypes we observed were concordant among the neuroinvasive viruses tested, suggesting that CC045 resistance likely results from a pan-flavivirus mechanism. However, we found that CC006 mice were highly susceptible to WNV and POWV but relatively resistant to JEV. Future studies will investigate the mechanism of JEV resistance in CC006 mice, potentially revealing disease mechanisms that are specific to JEV compared to other flaviviruses.

Host genes related to the antiviral immune response have been associated with the outcome of flavivirus infection in humans (16). For example, a common polymorphism that ablates expression of the chemokine receptor CCR5 (CCR5Δ32, best characterized because homozygotes are protected against HIV infection because CCR5 is the main co-receptor for HIV entry (60)) is associated with higher risk of WNV and TBEV symptomatic presentation and neuroinvasive disease (10, 14, 17, 18). A protective role for CCR5 against WNV and TBEV disease is consistent with studies showing that CCR5 deficient mice exhibit impaired trafficking of CD8 T cells necessary to clear flavivirus CNS infection (61-64). Furthermore, polymorphisms in the dsRNA sensors OAS1, OAS2, and OAS3 are associated with WNV and TBEV infection and neuroinvasive disease (10, 65, 66). Mechanistically, the SNP rs10774671 of OAS1 corresponds to a A>G change in a splice acceptor site, where the G allele (protective) generates the p46 isoform of OAS1. The p46 isoform is prenylated, localizes to flavivirus replication complexes on ER membranes, and inhibits WNV replication, whereas the p42 isoform (resulting from the A allele) is not prenylated and lacks antiviral activity (67). Among the 8 murine orthologs of OAS1, Oas1b

bioRxiv preprint doi: https://doi.org/10.1101/2022.10.24.513634; this version posted October 25, 2022. The copyright holder for this preprint (which was not certified by peer review) is the author/funder, who has granted bioRxiv a license to display the preprint in perpetuity. It is made available under aCC-BY-NC-ND 4.0 International license.

and Oas1g both encode a C-terminal CaaX domain homologous to the prenylation site in the p46 isoform of human OAS1 (67). But whereas Oas1b plays a dominant role restricting flavivirus pathogenesis in mice, we found no effect of Oas1g on survival after WNV or POWV infection. This could indicate that Oas1g is not important for controlling flavivirus infection, that the antiviral effects of Oas1g are not strong enough to affect lethality, or that the antiviral effects of Oas1g are not evident on the *Oas1b*^{null} C57BL/6J genetic background.

Polymorphisms within additional antiviral response genes (e.g., CD209/DC-SIGN, TLR3, IL-10) are associated with TBEV infection (11-15). Similarly, polymorphisms within antiviral response genes such as HERC5, IRF3, and MX1 are associated with WNV infection (10, 16, 68, 69). Other polymorphic host genes play a role in flavivirus infection, although their effect on human disease is less clear. TMEM41B is an ER-associated lipid scramblase that promotes replication of a wide variety of flaviviruses (including POWV, TBEV, and WNV) (70). TMEM41B is polymorphic in humans and TMEM41B alleles vary in their ability to support flavivirus replication in cell culture (70), although associations with the risk or outcome of flavivirus infection remain to be demonstrated.

Extensive studies using transgenic knockout mice have revealed the effects of various innate and adaptive immune genes on the pathogenesis of WNV and other flaviviruses (71) but investigating flavivirus pathogenesis in CC mice allows us to study complex traits and polymorphic alleles that better recapitulate the genetic diversity found in human populations (30, 33). A limitation of CC studies is that they can only reveal genetic factors that are polymorphic among the 8 CC founder lines (or private mutations that arose during the breeding of CC lines). Future studies will use F2 crosses of resistant

bioRxiv preprint doi: https://doi.org/10.1101/2022.10.24.513634; this version posted October 25, 2022. The copyright holder for this preprint (which was not certified by peer review) is the author/funder, who has granted bioRxiv a license to display the preprint in perpetuity. It is made available under aCC-BY-NC-ND 4.0 International license.

(e.g., CC045) and susceptible (e.g., CC071) CC lines and genetic mapping approaches to define the host genetic factors that contribute to the resistant phenotype of CC045 mice, analogous to previous studies that have used similar approaches to map QTL and underlying causal genes that contribute to host control of influenza A virus, SARS-CoV, SARS-CoV-2, and WNV (35, 37, 72-74).

Previous studies have used CC mice to investigate host genetic factors controlling WNV infection and pathogenesis (36, 37, 58, 75-77). These studies used F1 crosses of CC parental lines, so it is not straightforward to draw comparisons with the phenotypes we identified in CC parental lines. Further, our key lines of interest, CC045 and CC071, were not included in the earlier WNV studies. However, the QTL with the largest effect size identified in these studies mapped to *Oas1b* (36, 37). With this in mind, we designed our experiments to use only *Oas1b*^{null} CC lines, allowing us to identify other polymorphic genes that contribute to disease outcome. However, our design does not detect factors that are dependent upon or synergize with *Oas1b* for their activity. Since we expected *Oas1b*^{null} mice to be susceptible to neuroinvasive flaviviruses, the remarkable finding in our study was that CC045 mice were resistant to diverse neuroinvasive flaviviruses, even in the absence of Oas1b. We also identified other *Oas1b*^{null} CC lines (such as CC057) with more modest resistance phenotypes; future studies will investigate whether the resistant phenotype of CC057 mice derives from the same mechanism as CC045 mice. Notably, CC057 mice also were relatively resistant to RVFV, exhibiting a delayed disease course resulting in encephalitis rather than acute hepatitis (34). CC071 mice, which we identified as being highly susceptible to POWV, WNV, JEV, and SLEV previously have been found to be highly susceptible to SARS-CoV-2 (78) and RVFV (34) and were highly

bioRxiv preprint doi: https://doi.org/10.1101/2022.10.24.513634; this version posted October 25, 2022. The copyright holder for this preprint (which was not certified by peer review) is the author/funder, who has granted bioRxiv a license to display the preprint in perpetuity. It is made available under aCC-BY-NC-ND 4.0 International license.

susceptible to ZIKV when treated with an IFNAR1-blocking antibody (79). Altogether this suggests that CC mice can reveal immune mechanisms that control pathogenesis of diverse viruses.

In this study, we demonstrated that Oas1b restricts POWV pathogenesis, which was not surprising given that Oas1b has been shown to restrict all flaviviruses tested to date. Despite observing marked differences in survival between CC019-*Oas1b*^{del} and CC019 mice, we found no significant difference in WNV or POWV replication in CC019-*Oas1b*^{del} MEFs compared to CC019 MEFs, even though Oas1b has been shown to restrict flavivirus replication in MEFs derived from C3H.PRI-Flv^{r} mice (80). This discordance could be due to distinct genetic features of CC019 mice and differences between MEFs and other cell types. In this study, we also demonstrated the ability to generate genetic knockouts on a CC background (CC019-*Oas1b*^{del}), which will enable the study of the function of single genes in the context of genetically diverse mouse models.

Prevention of neuroinvasion could be achieved by one or more mechanisms, including a tighter BBB, modulated leukocyte trafficking into the CNS, and enhanced clearance of virus from the periphery. The data from the present study support a model of POWV pathogenesis in which persistent high levels of viremia increases the likelihood of virus stochastically breaching the BBB and accessing the CNS, where it leads to mortality. Thus, we propose that CC045 mice resist POWV infection by promoting the rapid clearance of POWV from the circulation and therefore limiting the opportunity for POWV neuroinvasion, and this effect is mediated by host factors outside of *Oas1b*. Future studies will investigate these non-*Oas1b* host factors using an F2 cross of susceptible

bioRxiv preprint doi: https://doi.org/10.1101/2022.10.24.513634; this version posted October 25, 2022. The copyright holder for this preprint (which was not certified by peer review) is the author/funder, who has granted bioRxiv a license to display the preprint in perpetuity. It is made available under aCC-BY-NC-ND 4.0 International license.

458 and resistant CC mice and use quantitative genetics approaches to identify polymorphic
459 genes that contribute to the resistant phenotype of CC045 mice.
460
461 **MATERIALS AND METHODS**
462
463 **Cells and viruses.** Vero (African green monkey kidney epithelial) cells were maintained
464 in Dulbecco's modified Eagle medium (DMEM) containing 5% heat-inactivated FBS at
465 37°C with 5% CO_2. POWV strains LB (Lineage I) and Spooner (DTV, Lineage II), WNV
466 strain NY2000, JEV strain Nakayama, and SLEV strain GHA-3 were provided by Dr.
467 Michael Diamond (Washington University in St. Louis). POWV strain MB5/12 (DTV,
468 Lineage II) was provided by Dr. Greg Ebel (Colorado State University). All viruses were
469 handled under BSL3 containment. Virus stocks were grown in Vero cells and titered by
470 focus-forming assay (FFA) (81). Duplicates of serial 10-fold dilutions of virus in growth
471 medium (DMEM containing 2% FBS and 20 mM HEPES) were applied to Vero cells in
472 96-well plates and incubated at 37°C with 5% CO_2. After 1 hour, cells were overlaid with
473 1% methylcellulose in minimum essential medium Eagle (MEM) containing 2% heat-
474 inactivated fetal bovine serum (FBS). Following incubation for approximately 24 hours
475 (WNV), 24-36 hours (JEV), or 48 hours (POWV and SLEV), plates were fixed with 2%
476 paraformaldehyde for 2 hours at room temperature. Fixed plates were incubated with 500
477 ng/ml flavivirus cross-reactive mouse MAb ZV13 (82) or E60 (83) for 2 hr at room
478 temperature or overnight at 4°C. After incubation at room temperature for 1 hr with a
479 1:2,500 dilution of horseradish peroxidase (HRP)-conjugated goat anti-mouse IgG

bioRxiv preprint doi: https://doi.org/10.1101/2022.10.24.513634; this version posted October 25, 2022. The copyright holder for this preprint (which was not certified by peer review) is the author/funder, who has granted bioRxiv a license to display the preprint in perpetuity. It is made available under aCC-BY-NC-ND 4.0 International license.

480 (Sigma), foci were detected by addition of TrueBlue substrate (KPL). Foci were quantified
481 with a CTL Immunospot instrument.
482
483 **Mice.** All mouse procedures were performed under protocols approved by the Institutional
484 Animal Care and Use Committee at the University of North Carolina at Chapel Hill. CC
485 mice were obtained from the UNC Systems Genetics Core Facility directly or as breeder
486 pairs that were mated in-house. C57BL/6J mice were bred in-house. *Oas1g*$^{-/-}$ mice were
487 obtained from Dr. Timothy Sheahan (UNC). All mouse work was performed under ABSL3
488 containment. Five-week-old or 9 to 12-week-old mice male and female mice were
489 inoculated in a volume of 50 µl by a subcutaneous (footpad) route. Mice received 100
490 FFU of POWV strain LB, MB5/12, or Spooner (DTV), WNV strain NY2000, JEV strain
491 Nakayama or SLEV strain GHA-3, diluted in HBSS with Ca^{2+} and Mg^{2+} supplemented
492 with 1% heat-inactivated FBS. Mice were monitored daily for disease signs for 21 days or
493 until the time of tissue harvest. Mice were euthanized upon reaching humane endpoints
494 including loss of ≥20% of starting weight, non-responsiveness, or severe neurological
495 disease signs (hunching, paralysis) interfering with the ability to access food and water;
496 euthanized mice were scored as dead the following day. To evaluate viremia, blood was
497 collected 2 dpi by submandibular bleed with a 5mm Goldenrod lancet, or by cardiac
498 puncture prior to perfusion in tissue harvest experiments.
499
500 **Generation of CC019-*Oas1b*^{del} mice.** CC019-*Oas1b*^{del} mice were generated through the
501 UNC Mutant Mouse Resource and Research Center, as part of a project to demonstrate
502 the feasibility of performing CRISPR/Cas9 genome editing in CC mice. The CC019 line

bioRxiv preprint doi: https://doi.org/10.1101/2022.10.24.513634; this version posted October 25, 2022. The copyright holder for this preprint (which was not certified by peer review) is the author/funder, who has granted bioRxiv a license to display the preprint in perpetuity. It is made available under aCC-BY-NC-ND 4.0 International license.

was chosen because it contains a functional *Oas1b* allele (derived from the WSB founder) and exhibited robust superovulation and in vitro fertilization (IVF) performance, with egg yields and embryo progression to the two-cell stage comparable to C57BL/6J mice. 4 CRISPR guide RNAs targeting the SNP position of the WSB allele were designed and validated. Two guide RNAs showed full activity *in vitro* and were chosen for microinjection. A donor oligonucleotide was designed to introduce the susceptible SNP plus additional silent mutations to disrupt Cas9 binding and cleavage of the introduced allele and to facilitate genotyping of the resulting animals. Microinjection conditions: Cas9 mRNA (20 or 40 ng/µl), 1 guide RNA (10 or 20 ng/µl) and donor oligonucleotide (20 or 50 ng/µl) were co-injected into the pronucleus of one-cell embryos produced by IVF. IVF/microinjection was performed for 3 days. The CC019 strain responded moderately to superovulation (average 8.3 eggs/female). IVF was successful on each of the 3 days, yielding a total of 358 injectable embryos (6.2/female). Injection survival and progression to the two-cell stage in vitro were comparable to C57BL/6J. However, production of live pups from injected embryos was low: only 2 live pups were produced from 280 implanted embryos. Both pups had CRISPR-induced mutations at the *Oas1b* locus. CC019-Oas1b^{del} mice are homozygous for a 12 base pair deletion in exon 4 of *Oas1b* which generates an in-frame 4 amino acid deletion. CC019-*Oas1b*^{del} mice were bred as knockout x knockout and exhibited similar breeding performance as the parental CC019 line. CC019-*Oas1b*^{del} mice were genotyped by generating a PCR amplicon from tail snip DNA using forward primer CCACACACAACCACCAGGAACC and reverse primer GGCTGTAGGACCTCATGTCAATCA, then sequencing with the forward primer TCTCATTGCCTTTCTCTTCTCAGTGTA. The wild-type sequence is

bioRxiv preprint doi: https://doi.org/10.1101/2022.10.24.513634; this version posted October 25, 2022. The copyright holder for this preprint (which was not certified by peer review) is the author/funder, who has granted bioRxiv a license to display the preprint in perpetuity. It is made available under aCC-BY-NC-ND 4.0 International license.

GGGAGTATGGGAGTCCGAGTAACTAAATTCAACACAGCCCAGGGCTTCCGAACCG TCTTGGAACTGGTCACCAAGTACAAACAGCTTCGAATCTACTGGACAGTGTATTAT GACTTTCGACATCAAGAGGTCTCTGAATACCTGCACCAA and the *Oas1b*^{del} sequence is

GGGAGTATGGGAGTCCGAGTAACTAAATTCAACACAGCCCAGGACTTGGAACTGG TCACCAAGTACAAACAGCTTCGAATCTACTGGACAGTGTATTATGACTTTCGACATC AAGAGGTCTCTGAATACCTGCACCAA.

Mouse Embryo Fibroblasts. Mouse embryo fibroblasts (MEFs) were prepared from E15 embryos. Pregnant mice were euthanized and the gravid uterus was isolated. Embryos were removed, placed in PBS, decapitated, and gut and liver were removed. Embryos were then minced with scalpels, trypsinized (1 ml per embryo), pipetted up and down with a 10 ml serological pipette to break up any chunks, and incubated for 5-10 min at room temperature. Cells were resuspended in DMEM supplemented with non-essential amino acids, L-Glutamine, Pen/Strep, and 10% heat-inactivated FBS and then pelleted by centrifugation at 1000 rpm for 5 min at 4°C. Supernatants were removed and cell pellets were resuspended in fresh media and pelleted again by centrifugation at 1000 rpm for 5 min at 4°C. Cell pellets were resuspended in 1 ml per embryo of fresh media and plated into culture flasks (1.5 embryos per T-150 flask) in 25 ml of fresh media and incubated at 37°C with 5% CO_2. After 24 hours, media was removed, cells were washed with 1X PBS, and fresh media was added. When monolayers reached near-confluency, MEFs were frozen down in DMEM supplemented with non-essential amino acids, L-Glutamine, Pen/Strep, 30% heat-inactivated FBS, and 20% DMSO and stored in liquid nitrogen.

bioRxiv preprint doi: https://doi.org/10.1101/2022.10.24.513634; this version posted October 25, 2022. The copyright holder for this preprint (which was not certified by peer review) is the author/funder, who has granted bioRxiv a license to display the preprint in perpetuity. It is made available under aCC-BY-NC-ND 4.0 International license.

549 Thawed MEFs were seeded in 6-well plates at 2 x 10^5 cells per well in DMEM
550 supplemented with non-essential amino acids, L-Glutamine, Pen/Strep, and 10% heat-
551 inactivated FBS. MEFs were infected at an MOI of 0.01 with POWV strain LB or WNV
552 strain NY2000. After 1 hour, inoculum was removed and replaced with fresh media and
553 plates were incubated at 37°C with 5% CO_2. After 4, 24, 48, or 72 hours, supernatants
554 were collected and titered by focus-forming assay on Vero cells.
555
556 **Bone-marrow derived macrophages.** Bone marrow-derived macrophages (BMDM)
557 were generated from CC mice. Mice were euthanized and femurs and tibias were isolated
558 from hind limbs. Bone marrow was flushed out with 10 ml DMEM delivered via syringe
559 with 25G ½ inch needle. Bone marrow was pooled and pipetted up and down with a 5 ml
560 serological pipette to break up large chunks. Cells were pelleted by centrifugation at 1500
561 rpm for 5 min at 4°C. Supernatants were removed and cell pellets were resuspended in
562 ACK Red Blood Cell Lysis Buffer containing 150 mM NH_4Cl, 10 mM $KHCO_3$, and 0.1 mM
563 EDTA pH 7.3, and incubated for 2-3 minutes. Cells were resuspended in DMEM
564 containing 10% heat-inactivated FBS and then pelleted by centrifugation at 1500 rpm for
565 5 min at 4°C. Cell pellets were resuspended in DMEM containing 10% heat-inactivated
566 FBS and counted. 12-well non-TC treated plates were seeded with 1.5 x 10^5 cells/well in
567 1 ml of DMEM containing L-Glutamine, NaPyr, Pen/Strep, 10% heat-inactivated FBS, and
568 40 ng/ml mouse M-CSF (BioLegend 576406) and incubated for 7 days at 37°C with 5%
569 CO_2. BMDMs were infected at an MOI of 0.01 with POWV strain MB5/12 or WNV strain
570 NY2000 in DMEM containing L-Glutamine, NaPyr, Pen/Strep, 10% heat-inactivated FBS,
571 and 20 ng/ml mouse M-CSF. After 1 hour, inoculum was removed and replaced with fresh

bioRxiv preprint doi: https://doi.org/10.1101/2022.10.24.513634; this version posted October 25, 2022. The copyright holder for this preprint (which was not certified by peer review) is the author/funder, who has granted bioRxiv a license to display the preprint in perpetuity. It is made available under aCC-BY-NC-ND 4.0 International license.

media and plates were incubated at 37°C with 5% CO_2. After 4, 24, 48, or 72 hours, supernatants were collected and titered by focus-forming assay on Vero cells.

Measurement of Viremia. Blood was collected from mice by submandibular bleed or terminal cardiac puncture in serum separator tubes (BD). Serum was separated by centrifugation for 8000 rpm for 4 min and stored at -80°C until RNA isolation. RNA was extracted with the Viral RNA Mini Kit (Qiagen). Viral RNA levels were determined by TaqMan one-step qRT-PCR on a CFX96 Touch Real-Time PCR Detection System (BioRad) using standard cycling conditions. Viremia is expressed on a Log_{10} scale as copies per ml based on a standard curve produced using serial 10-fold dilutions of a DNA plasmid containing a 400 bp gBlock (Integrated DNA Technologies) encoding a portion of the viral envelope (E) protein sequence. All primers and probes were purchased from Integrated DNA Technologies. Primers used to detect POWV MB5/12 were: forward, GAAGCTGAAAGGCACAACTTAC; reverse, CACCTCCATGACCACTGTATC; and probe, AAGAGTTCCTGTGGACAGTGGTCA. Primers used to detect WNV NY2000 were: forward, TCAGCGATCTCTCCACCAAAG; reverse, GGGTCAGCACGTTTGTCATTG; and probe, TGCCCGACCATGGGAGAAGCTC. Primers used to detect JEV Nakayama were: forward, CAGCGTGGAGAAACAGAGAA; reverse, TGTGACCCAAGAGCAACAA; and probe, CATGGAATTTGAAGAGGCGCACGC.

Tissue Titers. Nine to twelve-week-old male and female mice were infected with 100 FFU of POWV strain MB5/12. At 3 or 7 dpi, mice were bled by cardiac puncture, perfused

bioRxiv preprint doi: https://doi.org/10.1101/2022.10.24.513634; this version posted October 25, 2022. The copyright holder for this preprint (which was not certified by peer review) is the author/funder, who has granted bioRxiv a license to display the preprint in perpetuity. It is made available under aCC-BY-NC-ND 4.0 International license.

595 with 20 ml of PBS, and tissues were harvested. Brains and spleens were collected into 2
596 ml screwcap tubes containing 1 ml of DMEM supplemented with 2% heat-inactivated FBS
597 and homogenizer beads. Tissues were stored at -80°C until processing. Tissues were
598 thawed and homogenized using a MagNA Lyser (Roche) set to 6000 for 1 min.
599 Homogenates were titered by plaque assay on Vero cells. Serial 10-fold dilutions of tissue
600 homogenates were applied to Vero cells in 6-well plates and incubated at 37°C with 5%
601 CO_2. After 1 hour, cells were overlaid with 1% methylcellulose in minimum essential
602 medium Eagle (MEM) containing 2% heat-inactivated FBS. Following incubation for 6
603 days, plates were fixed with 2% paraformaldehyde overnight at room temperature. Fixed
604 plates were stained with 1% crystal violet in 20% ethanol, washed with tap water, and
605 plaques were counted manually.
606
607 **Data analysis.** Data were analyzed with GraphPad Prism software. Growth curves were
608 analyzed by two-way ANOVA to assess the impact of time and CC line on viral replication,
609 compared to CC019-*Oas1b*^{del} (Fig.1E-F) or CC045 (Fig. 5). Viremia was compared to
610 CC045 mice by one-way ANOVA (Fig. 4). Tissue titers were analyzed by two-way ANOVA
611 to assess the impact of time and CC line on viral loads, compared to CC045 (Fig. 6). A p
612 value of < 0.05 was considered statistically significant.
613
614 **ACKNOWLEDGEMENTS**
615 This work was supported by R21 AI145377 (H.M.L), R01 AI170625 (H.M.L.), and U19
616 AI100625 (M.T.H. and M.T.F.), by start-up funds from the UNC Lineberger
617 Comprehensive Cancer Center and Department of Microbiology & Immunology, and by

bioRxiv preprint doi: https://doi.org/10.1101/2022.10.24.513634; this version posted October 25, 2022. The copyright holder for this preprint (which was not certified by peer review) is the author/funder, who has granted bioRxiv a license to display the preprint in perpetuity. It is made available under aCC-BY-NC-ND 4.0 International license.

Systems Genetics Pilot Projects from the UNC School of Medicine. B.A.J. was supported by F32 AI161786. K.E.N. was supported by T32 AI007419. We appreciate the support of the Systems Genetics Core Facility and Mutant Mouse Research and Resource Center and we also acknowledge Dr. Dale Cowley and the UNC Animal Models Core Facility for generating the CC019-*Oas1b*^{del} mice.

REFERENCES

1. Gould EA, Solomon T. 2008. Pathogenic flaviviruses. Lancet 371:500-9.
2. Solomon T. 2004. Flavivirus encephalitis. N Engl J Med 351:370-8.
3. Hermance ME, Thangamani S. 2017. Powassan Virus: An Emerging Arbovirus of Public Health Concern in North America. Vector Borne Zoonotic Dis 17:453-462.
4. Paules CI, Marston HD, Bloom ME, Fauci AS. 2018. Tickborne Diseases - Confronting a Growing Threat. N Engl J Med 379:701-703.
5. McLean DM, Donohue WL. 1959. Powassan virus: isolation of virus from a fatal case of encephalitis. Can Med Assoc J 80:708-11.
6. Beasley DW, Suderman MT, Holbrook MR, Barrett AD. 2001. Nucleotide sequencing and serological evidence that the recently recognized deer tick virus is a genotype of Powassan virus. Virus Res 79:81-9.
7. Kuno G, Artsob H, Karabatsos N, Tsuchiya KR, Chang GJ. 2001. Genomic sequencing of deer tick virus and phylogeny of powassan-related viruses of North America. Am J Trop Med Hyg 65:671-6.
8. Ebel GD, Spielman A, Telford SR. 2001. Phylogeny of North American Powassan virus. J Gen Virol 82:1657-1665.
9. Ebel GD. 2010. Update on Powassan virus: emergence of a North American tick-borne flavivirus. Annu Rev Entomol 55:95-110.
10. Bigham AW, Buckingham KJ, Husain S, Emond MJ, Bofferding KM, Gildersleeve H, Rutherford A, Astakhova NM, Perelygin AA, Busch MP, Murray KO, Sejvar JJ, Green S, Kriesel J, Brinton MA, Bamshad M. 2011. Host genetic risk factors for West Nile virus infection and disease progression. PLoS One 6:e24745.
11. Barkhash AV, Babenko VN, Voevoda MI, Romaschenko AG. 2016. Association of IL28B and IL10 gene polymorphism with predisposition to tick-borne encephalitis in a Russian population. Ticks Tick Borne Dis 7:808-812.
12. Barkhash AV, Perelygin AA, Babenko VN, Brinton MA, Voevoda MI. 2012. Single nucleotide polymorphism in the promoter region of the CD209 gene is associated with human predisposition to severe forms of tick-borne encephalitis. Antiviral Res 93:64-8.
13. Barkhash AV, Voevoda MI, Romaschenko AG. 2013. Association of single nucleotide polymorphism rs3775291 in the coding region of the TLR3 gene with predisposition to tick-borne encephalitis in a Russian population. Antiviral Res 99:136-8.

bioRxiv preprint doi: https://doi.org/10.1101/2022.10.24.513634; this version posted October 25, 2022. The copyright holder for this preprint (which was not certified by peer review) is the author/funder, who has granted bioRxiv a license to display the preprint in perpetuity. It is made available under aCC-BY-NC-ND 4.0 International license.

14. Kindberg E, Mickiene A, Ax C, Akerlind B, Vene S, Lindquist L, Lundkvist A, Svensson L. 2008. A deletion in the chemokine receptor 5 (CCR5) gene is associated with tickborne encephalitis. J Infect Dis 197:266-9.
15. Mickiene A, Pakalniene J, Nordgren J, Carlsson B, Hagbom M, Svensson L, Lindquist L. 2014. Polymorphisms in chemokine receptor 5 and Toll-like receptor 3 genes are risk factors for clinical tick-borne encephalitis in the Lithuanian population. PLoS One 9:e106798.
16. Cahill ME, Conley S, DeWan AT, Montgomery RR. 2018. Identification of genetic variants associated with dengue or West Nile virus disease: a systematic review and meta-analysis. BMC Infect Dis 18:282.
17. Glass WG, McDermott DH, Lim JK, Lekhong S, Yu SF, Frank WA, Pape J, Cheshier RC, Murphy PM. 2006. CCR5 deficiency increases risk of symptomatic West Nile virus infection. J Exp Med 203:35-40.
18. Lim JK, McDermott DH, Lisco A, Foster GA, Krysztof D, Follmann D, Stramer SL, Murphy PM. 2010. CCR5 deficiency is a risk factor for early clinical manifestations of West Nile virus infection but not for viral transmission. J Infect Dis 201:178-85.
19. Webster LT. 1937. Inheritance of Resistance of Mice to Enteric Bacterial and Neurotropic Virus Infections. J Exp Med 65:261-86.
20. Perelygin AA, Scherbik SV, Zhulin IB, Stockman BM, Li Y, Brinton MA. 2002. Positional cloning of the murine flavivirus resistance gene. Proc Natl Acad Sci U S A 99:9322-7.
21. Mashimo T, Lucas M, Simon-Chazottes D, Frenkiel MP, Montagutelli X, Ceccaldi PE, Deubel V, Guenet JL, Despres P. 2002. A nonsense mutation in the gene encoding 2'-5'-oligoadenylate synthetase/L1 isoform is associated with West Nile virus susceptibility in laboratory mice. Proc Natl Acad Sci U S A 99:11311-6.
22. Webster LT. 1933. Inherited and Acquired Factors in Resistance to Infection : I. Development of Resistant and Susceptible Lines of Mice through Selective Breeding. J Exp Med 57:793-817.
23. Casals J, Schneider HA. 1943. Natural Resistance and Susceptibility to Russian Spring-Summer Encephalitis in Mice. Proceedings of the Society for Experimental Biology and Medicine 54:201-202.
24. Webster LT, Clow AD. 1936. Experimental Encephalitis (St. Louis Type) in Mice with High Inborn Resistance : A Chronic Subclinical Infection. J Exp Med 63:827-45.
25. Webster LT, Johnson MS. 1941. Comparative Virulence of St. Louis Encephalitis Virus Cultured with Brain Tissue from Innately Susceptible and Innately Resistant Mice. J Exp Med 74:489-94.
26. Sawyer WA, Lloyd W. 1931. The Use of Mice in Tests of Immunity against Yellow Fever. J Exp Med 54:533-55.
27. Lynch CJ, Hughes TP. 1936. The Inheritance of Susceptibility to Yellow Fever Encephalitis in Mice. Genetics 21:104-12.
28. Brinton MA, Perelygin AA. 2003. Genetic resistance to flaviviruses. Adv Virus Res 60:43-85.
29. Collaborative Cross C. 2012. The genome architecture of the Collaborative Cross mouse genetic reference population. Genetics 190:389-401.

bioRxiv preprint doi: https://doi.org/10.1101/2022.10.24.513634; this version posted October 25, 2022. The copyright holder for this preprint (which was not certified by peer review) is the author/funder, who has granted bioRxiv a license to display the preprint in perpetuity. It is made available under aCC-BY-NC-ND 4.0 International license.

30. Noll KE, Ferris MT, Heise MT. 2019. The Collaborative Cross: A Systems Genetics Resource for Studying Host-Pathogen Interactions. Cell Host Microbe 25:484-498.
31. Srivastava A, Morgan AP, Najarian ML, Sarsani VK, Sigmon JS, Shorter JR, Kashfeen A, McMullan RC, Williams LH, Giusti-Rodriguez P, Ferris MT, Sullivan P, Hock P, Miller DR, Bell TA, McMillan L, Churchill GA, de Villena FP. 2017. Genomes of the Mouse Collaborative Cross. Genetics 206:537-556.
32. Graham JB, Swarts JL, Mooney M, Choonoo G, Jeng S, Miller DR, Ferris MT, McWeeney S, Lund JM. 2017. Extensive Homeostatic T Cell Phenotypic Variation within the Collaborative Cross. Cell Rep 21:2313-2325.
33. Leist SR, Baric RS. 2018. Giving the Genes a Shuffle: Using Natural Variation to Understand Host Genetic Contributions to Viral Infections. Trends Genet 34:777-789.
34. Cartwright HN, Barbeau DJ, Doyle JD, Klein E, Heise MT, Ferris MT, McElroy AK. 2022. Genetic diversity of collaborative cross mice enables identification of novel rift valley fever virus encephalitis model. PLoS Pathog 18:e1010649.
35. Schafer A, Leist SR, Gralinski LE, Martinez DR, Winkler ES, Okuda K, Hawkins PE, Gully KL, Graham RL, Scobey DT, Bell TA, Hock P, Shaw GD, Loome JF, Madden EA, Anderson E, Baxter VK, Taft-Benz SA, Zweigart MR, May SR, Dong S, Clark M, Miller DR, Lynch RM, Heise MT, Tisch R, Boucher RC, Pardo Manuel de Villena F, Montgomery SA, Diamond MS, Ferris MT, Baric RS. 2022. A Multitrait Locus Regulates Sarbecovirus Pathogenesis. mBio 13:e0145422.
36. Graham JB, Thomas S, Swarts J, McMillan AA, Ferris MT, Suthar MS, Treuting PM, Ireton R, Gale M, Jr., Lund JM. 2015. Genetic diversity in the collaborative cross model recapitulates human West Nile virus disease outcomes. mBio 6:e00493-15.
37. Green R, Wilkins C, Thomas S, Sekine A, Hendrick DM, Voss K, Ireton RC, Mooney M, Go JT, Choonoo G, Jeng S, de Villena FP, Ferris MT, McWeeney S, Gale M, Jr. 2017. Oas1b-dependent Immune Transcriptional Profiles of West Nile Virus Infection in the Collaborative Cross. G3 (Bethesda) 7:1665-1682.
38. Elbahesh H, Jha BK, Silverman RH, Scherbik SV, Brinton MA. 2011. The Flvr-encoded murine oligoadenylate synthetase 1b (Oas1b) suppresses 2-5A synthesis in intact cells. Virology 409:262-70.
39. Kakuta S, Shibata S, Iwakura Y. 2002. Genomic structure of the mouse 2',5'-oligoadenylate synthetase gene family. J Interferon Cytokine Res 22:981-93.
40. Kemenesi G, Banyai K. 2019. Tick-Borne Flaviviruses, with a Focus on Powassan Virus. Clin Microbiol Rev 32.
41. Campbell GL, Hills SL, Fischer M, Jacobson JA, Hoke CH, Hombach JM, Marfin AA, Solomon T, Tsai TF, Tsu VD, Ginsburg AS. 2011. Estimated global incidence of Japanese encephalitis: a systematic review. Bull World Health Organ 89:766-74, 774A-774E.
42. Heffelfinger JD, Li X, Batmunkh N, Grabovac V, Diorditsa S, Liyanage JB, Pattamadilok S, Bahl S, Vannice KS, Hyde TB, Chu SY, Fox KK, Hills SL, Marfin AA. 2017. Japanese Encephalitis Surveillance and Immunization - Asia and Western Pacific Regions, 2016. MMWR Morb Mortal Wkly Rep 66:579-583.

bioRxiv preprint doi: https://doi.org/10.1101/2022.10.24.513634; this version posted October 25, 2022. The copyright holder for this preprint (which was not certified by peer review) is the author/funder, who has granted bioRxiv a license to display the preprint in perpetuity. It is made available under aCC-BY-NC-ND 4.0 International license.

43. Furuya-Kanamori L, Gyawali N, Mills DJ, Hugo LE, Devine GJ, Lau CL. 2022. The Emergence of Japanese Encephalitis in Australia and the Implications for a Vaccination Strategy. Trop Med Infect Dis 7.
44. Centers for Disease Control and Prevention. West Nile Virus: Final Cumulative Maps & Data for 1999– 2020 [updated December 17, 2021]. https://www.cdc.gov/westnile/statsmaps/cumMapsData.html. Accessed
45. Lindquist L, Vapalahti O. 2008. Tick-borne encephalitis. Lancet 371:1861-71.
46. Heinz FX, Stiasny K, Holzmann H, Grgic-Vitek M, Kriz B, Essl A, Kundi M. 2013. Vaccination and tick-borne encephalitis, central Europe. Emerg Infect Dis 19:69-76.
47. Roesch F, Fajardo A, Moratorio G, Vignuzzi M. 2019. Usutu Virus: An Arbovirus on the Rise. Viruses 11.
48. Cle M, Beck C, Salinas S, Lecollinet S, Gutierrez S, Van de Perre P, Baldet T, Foulongne V, Simonin Y. 2019. Usutu virus: A new threat? Epidemiol Infect 147:e232.
49. Shives KD, Tyler KL, Beckham JD. 2017. Molecular mechanisms of neuroinflammation and injury during acute viral encephalitis. J Neuroimmunol 308:102-111.
50. Milora KA, Rall GF. 2019. Interferon Control of Neurotropic Viral Infections. Trends Immunol 40:842-856.
51. Klein RS, Hunter CA. 2017. Protective and Pathological Immunity during Central Nervous System Infections. Immunity 46:891-909.
52. Klein RS, Garber C, Howard N. 2017. Infectious immunity in the central nervous system and brain function. Nat Immunol 18:132-141.
53. Stone ET, Hassert M, Geerling E, Wagner C, Brien JD, Ebel GD, Hirsch AJ, German C, Smith JL, Pinto AK. 2022. Balanced T and B cell responses are required for immune protection against Powassan virus in virus-like particle vaccination. Cell Rep 38:110388.
54. Santos RI, Hermance ME, Reynolds ES, Thangamani S. 2021. Salivary gland extract from the deer tick, Ixodes scapularis, facilitates neuroinvasion by Powassan virus in BALB/c mice. Sci Rep 11:20873.
55. Mlera L, Meade-White K, Saturday G, Scott D, Bloom ME. 2017. Modeling Powassan virus infection in Peromyscus leucopus, a natural host. PLoS Negl Trop Dis 11:e0005346.
56. Hermance ME, Thangamani S. 2015. Tick Saliva Enhances Powassan Virus Transmission to the Host, Influencing Its Dissemination and the Course of Disease. J Virol 89:7852-60.
57. Pesko KN, Torres-Perez F, Hjelle BL, Ebel GD. 2010. Molecular epidemiology of Powassan virus in North America. J Gen Virol 91:2698-705.
58. Graham JB, Swarts JL, Wilkins C, Thomas S, Green R, Sekine A, Voss KM, Ireton RC, Mooney M, Choonoo G, Miller DR, Treuting PM, Pardo Manuel de Villena F, Ferris MT, McWeeney S, Gale M, Jr., Lund JM. 2016. A Mouse Model of Chronic West Nile Virus Disease. PLoS Pathog 12:e1005996.
59. Cain MD, Salimi H, Diamond MS, Klein RS. 2019. Mechanisms of Pathogen Invasion into the Central Nervous System. Neuron 103:771-783.

bioRxiv preprint doi: https://doi.org/10.1101/2022.10.24.513634; this version posted October 25, 2022. The copyright holder for this preprint (which was not certified by peer review) is the author/funder, who has granted bioRxiv a license to display the preprint in perpetuity. It is made available under aCC-BY-NC-ND 4.0 International license.

60. Lopalco L. 2010. CCR5: From Natural Resistance to a New Anti-HIV Strategy. Viruses 2:574-600.
61. Glass WG, Lim JK, Cholera R, Pletnev AG, Gao JL, Murphy PM. 2005. Chemokine receptor CCR5 promotes leukocyte trafficking to the brain and survival in West Nile virus infection. J Exp Med 202:1087-98.
62. Larena M, Regner M, Lobigs M. 2012. The chemokine receptor CCR5, a therapeutic target for HIV/AIDS antagonists, is critical for recovery in a mouse model of Japanese encephalitis. PLoS One 7:e44834.
63. Durrant DM, Daniels BP, Pasieka T, Dorsey D, Klein RS. 2015. CCR5 limits cortical viral loads during West Nile virus infection of the central nervous system. J Neuroinflammation 12:233.
64. Michlmayr D, Bardina SV, Rodriguez CA, Pletnev AG, Lim JK. 2016. Dual Function of Ccr5 during Langat Virus Encephalitis: Reduction in Neutrophil-Mediated Central Nervous System Inflammation and Increase in T Cell-Mediated Viral Clearance. J Immunol 196:4622-31.
65. Lim JK, Lisco A, McDermott DH, Huynh L, Ward JM, Johnson B, Johnson H, Pape J, Foster GA, Krysztof D, Follmann D, Stramer SL, Margolis LB, Murphy PM. 2009. Genetic variation in OAS1 is a risk factor for initial infection with West Nile virus in man. PLoS Pathog 5:e1000321.
66. Barkhash AV, Perelygin AA, Babenko VN, Myasnikova NG, Pilipenko PI, Romaschenko AG, Voevoda MI, Brinton MA. 2010. Variability in the 2'-5'-oligoadenylate synthetase gene cluster is associated with human predisposition to tick-borne encephalitis virus-induced disease. J Infect Dis 202:1813-8.
67. Soveg FW, Schwerk J, Gokhale NS, Cerosaletti K, Smith JR, Pairo-Castineira E, Kell AM, Forero A, Zaver SA, Esser-Nobis K, Roby JA, Hsiang TY, Ozarkar S, Clingan JM, McAnarney ET, Stone AE, Malhotra U, Speake C, Perez J, Balu C, Allenspach EJ, Hyde JL, Menachery VD, Sarkar SN, Woodward JJ, Stetson DB, Baillie JK, Buckner JH, Gale M, Jr., Savan R. 2021. Endomembrane targeting of human OAS1 p46 augments antiviral activity. Elife 10.
68. Danial-Farran N, Eghbaria S, Schwartz N, Kra-Oz Z, Bisharat N. 2015. Genetic variants associated with susceptibility of Ashkenazi Jews to West Nile virus infection. Epidemiol Infect 143:857-63.
69. Long D, Deng X, Singh P, Loeb M, Lauring AS, Seielstad M. 2016. Identification of genetic variants associated with susceptibility to West Nile virus neuroinvasive disease. Genes Immun 17:298-304.
70. Hoffmann HH, Schneider WM, Rozen-Gagnon K, Miles LA, Schuster F, Razooky B, Jacobson E, Wu X, Yi S, Rudin CM, MacDonald MR, McMullan LK, Poirier JT, Rice CM. 2021. TMEM41B Is a Pan-flavivirus Host Factor. Cell 184:133-148 e20.
71. Manet C, Roth C, Tawfik A, Cantaert T, Sakuntabhai A, Montagutelli X. 2018. Host genetic control of mosquito-borne Flavivirus infections. Mamm Genome 29:384-407.
72. Ferris MT, Aylor DL, Bottomly D, Whitmore AC, Aicher LD, Bell TA, Bradel-Tretheway B, Bryan JT, Buus RJ, Gralinski LE, Haagmans BL, McMillan L, Miller DR, Rosenzweig E, Valdar W, Wang J, Churchill GA, Threadgill DW, McWeeney SK, Katze MG, Pardo-Manuel de Villena F, Baric RS, Heise MT. 2013. Modeling

bioRxiv preprint doi: https://doi.org/10.1101/2022.10.24.513634; this version posted October 25, 2022. The copyright holder for this preprint (which was not certified by peer review) is the author/funder, who has granted bioRxiv a license to display the preprint in perpetuity. It is made available under aCC-BY-NC-ND 4.0 International license.

host genetic regulation of influenza pathogenesis in the collaborative cross. PLoS Pathog 9:e1003196.

73. Gralinski LE, Ferris MT, Aylor DL, Whitmore AC, Green R, Frieman MB, Deming D, Menachery VD, Miller DR, Buus RJ, Bell TA, Churchill GA, Threadgill DW, Katze MG, McMillan L, Valdar W, Heise MT, Pardo-Manuel de Villena F, Baric RS. 2015. Genome Wide Identification of SARS-CoV Susceptibility Loci Using the Collaborative Cross. PLoS Genet 11:e1005504.

74. Maurizio PL, Ferris MT, Keele GR, Miller DR, Shaw GD, Whitmore AC, West A, Morrison CR, Noll KE, Plante KS, Cockrell AS, Threadgill DW, Pardo-Manuel de Villena F, Baric RS, Heise MT, Valdar W. 2018. Bayesian Diallel Analysis Reveals Mx1-Dependent and Mx1-Independent Effects on Response to Influenza A Virus in Mice. G3 (Bethesda) 8:427-445.

75. Green R, Wilkins C, Thomas S, Sekine A, Ireton RC, Ferris MT, Hendrick DM, Voss K, de Villena FP, Baric R, Heise M, Gale M, Jr. 2016. Identifying protective host gene expression signatures within the spleen during West Nile virus infection in the collaborative cross model. Genom Data 10:114-117.

76. Green R, Wilkins C, Thomas S, Sekine A, Ireton RC, Ferris MT, Hendrick DM, Voss K, Pardo-Manuel de Villena F, Baric RS, Heise MT, Gale M, Jr. 2016. Transcriptional profiles of WNV neurovirulence in a genetically diverse Collaborative Cross population. Genom Data 10:137-140.

77. Graham JB, Swarts JL, Menachery VD, Gralinski LE, Schafer A, Plante KS, Morrison CR, Voss KM, Green R, Choonoo G, Jeng S, Miller DR, Mooney MA, McWeeney SK, Ferris MT, Pardo-Manuel de Villena F, Gale M, Heise MT, Baric RS, Lund JM. 2020. Immune Predictors of Mortality After Ribonucleic Acid Virus Infection. J Infect Dis 221:882-889.

78. Montagutelli X, Prot M, Jouvion G, Levillayer L, Conquet L, Reyes-Gomez E, Donati F, Albert M, van der Werf S, Jaubert J, Simon-Lorière E. 2021. A mouse-adapted SARS-CoV-2 strain replicating in standard laboratory mice. bioRxiv doi:10.1101/2021.07.10.451880:2021.07.10.451880.

79. Manet C, Simon-Loriere E, Jouvion G, Hardy D, Prot M, Conquet L, Flamand M, Panthier JJ, Sakuntabhai A, Montagutelli X. 2020. Genetic Diversity of Collaborative Cross Mice Controls Viral Replication, Clinical Severity, and Brain Pathology Induced by Zika Virus Infection, Independently of Oas1b. J Virol 94.

80. Scherbik SV, Paranjape JM, Stockman BM, Silverman RH, Brinton MA. 2006. RNase L plays a role in the antiviral response to West Nile virus. J Virol 80:2987-99.

81. Brien JD, Lazear HM, Diamond MS. 2013. Propagation, quantification, detection, and storage of West Nile virus. Curr Protoc Microbiol 31:15D 3 1-15D 3 18.

82. Zhao H, Fernandez E, Dowd KA, Speer SD, Platt DJ, Gorman MJ, Govero J, Nelson CA, Pierson TC, Diamond MS, Fremont DH. 2016. Structural Basis of Zika Virus-Specific Antibody Protection. Cell 166:1016-1027.

83. Oliphant T, Nybakken GE, Engle M, Xu Q, Nelson CA, Sukupolvi-Petty S, Marri A, Lachmi BE, Olshevsky U, Fremont DH, Pierson TC, Diamond MS. 2006. Antibody recognition and neutralization determinants on domains I and II of West Nile Virus envelope protein. J Virol 80:12149-59.

bioRxiv preprint doi: https://doi.org/10.1101/2022.10.24.513634; this version posted October 25, 2022. The copyright holder for this preprint (which was not certified by peer review) is the author/funder, who has granted bioRxiv a license to display the preprint in perpetuity. It is made available under aCC-BY-NC-ND 4.0 International license.

884

885 **FIGURE LEGENDS**

886

887 **Figure 1. Oas1b restricts pathogenesis of diverse neuroinvasive flaviviruses.** A-D.
888 Five to six-week-old male and female CC019, CC019-*Oas1b*^{del}, or C57BL/6J mice were
889 infected with 100 FFU of POWV strain LB (A), POWV DTV strain Spooner (B), WNV strain
890 NY2000 (C), or JEV strain Nakayama (D) by subcutaneous inoculation in the footpad and
891 lethality was monitored for 21 days. Data are combined from 4-5 experiments per virus.
892 E-F. Mouse embryo fibroblasts (MEFs) were harvested from the indicated mouse lines
893 for multistep growth curve analysis. MEFs were infected at an MOI of 0.01 with POWV
894 strain LB (E) or WNV strain NY2000 (F). Supernatants were collected at 4, 24, 48, or 72
895 hours post-infection and titered by focus-forming assay on Vero cells. Results shown are
896 the mean +/- SEM of 2-3 independent experiments performed in duplicate or triplicate.
897 Asterisks represent statistical significance (* $p<0.05$, ** $p<0.01$, *** $p<0.001$) by two-way
898 ANOVA compared to CC019-*Oas1b*^{del}. G-H. Nine to twelve-week-old C57BL/6J wild-type
899 or *Oas1g*$^{-/-}$ male and female mice were infected with 100 FFU of POWV strain MB5/12
900 (G) or WNV strain NY2000 (H) by subcutaneous inoculation in the footpad and lethality
901 was monitored for 21 days.

902

903 **Figure 2. Host factors influence POWV pathogenesis across Oas1b-null**
904 **Collaborative Cross mouse lines.** Nine to twelve-week-old male and female mice were
905 infected with 100 FFU of POWV (strain LB) by subcutaneous inoculation in the footpad
906 and lethality was monitored for 21 days. Lines are ordered by percent survival and mean

bioRxiv preprint doi: https://doi.org/10.1101/2022.10.24.513634; this version posted October 25, 2022. The copyright holder for this preprint (which was not certified by peer review) is the author/funder, who has granted bioRxiv a license to display the preprint in perpetuity. It is made available under aCC-BY-NC-ND 4.0 International license.

907 time to death. N=34 C67BL/6 mice, 18 CC019-*Oas1b*^{del} mice, and 6-7 mice for other lines.
908 Data are combined from 9 experiments.
909
910 **Figure 3. Susceptibility phenotypes in Collaborative Cross mice are shared among**
911 **diverse neuroinvasive flaviviruses.** A-D. Nine to twelve-week-old male and female
912 mice from *Oas1b*-null CC lines were infected with 100 FFU of POWV strain MB5/12 (A),
913 WNV strain NY2000 (B), JEV strain Nakayama (C), or SLEV strain GHA-3 (D) by
914 subcutaneous inoculation in the footpad and lethality was monitored for 21 days. Data
915 are combined from 4-8 experiments per virus. E. Nine to twelve-week-old male mice from
916 *Oas1b*$^{+/+}$ CC lines were infected with 100 FFU of POWV strain MB5/12 and lethality was
917 monitored for 21 days. Data represent a single experiment.
918
919 **Figure 4. Serum viral loads at 2 dpi do not correlate with susceptibility to**
920 **neuroinvasive flaviviruses.** Nine to twelve-week-old male and female mice were
921 infected with 100 FFU of POWV (A and B), WNV (C), or JEV (D) by subcutaneous
922 inoculation in the footpad. Mice were bled 2 dpi and viremia was assessed by qRT-PCR.
923 Asterisks represent statistical significance (* $p<0.05$, *** $p<0.001$) by one-way ANOVA
924 compared to CC045 (panels A, C, and D). CC lines in A, C, and D are all *Oas1b*-null; CC
925 lines in B are *Oas1b*$^{+/+}$. Open symbols denote surviving mice.
926
927 **Figure 5. Susceptibility to flavivirus disease is concordant with restriction of viral**
928 **replication in macrophages ex vivo.** Bone marrow-derived macrophages (BMDM) were
929 harvested from CC mice (CC045, CC071, and CC015) for multistep growth curve

bioRxiv preprint doi: https://doi.org/10.1101/2022.10.24.513634; this version posted October 25, 2022. The copyright holder for this preprint (which was not certified by peer review) is the author/funder, who has granted bioRxiv a license to display the preprint in perpetuity. It is made available under aCC-BY-NC-ND 4.0 International license.

930 analysis. BMDMs were infected at an MOI of 0.01 with POWV (A) or WNV (B).
931 Supernatants were collected at 4, 24, 48, or 72 hours post-infection and titered by focus-
932 forming assay on Vero cells. Results shown are the mean +/- SEM of 2-3 independent
933 experiments performed in duplicate or triplicate. Asterisks represent statistical
934 significance (* $p<0.05$, *** $p<0.001$) by two-way ANOVA compared to CC045.
935
936 **Figure 6. Reduced CNS viral loads correlate with POWV resistance.** Nine to twelve-
937 week-old male and female CC071 (susceptible) and CC045 (resistant) mice were infected
938 with 100 FFU of POWV (strain MB5/12) by subcutaneous inoculation in the footpad. A-D.
939 At the indicated time points, mice were perfused and tissues were harvested. A. Mice
940 were bled by cardiac puncture prior to perfusion and viremia was assessed by qRT-PCR.
941 B-D. Spleen, brain, and spinal cord homogenates were titered by plaque assay on Vero
942 cells. E-F. Mice were serially bled 2, 3, and 4 dpi and viremia was assessed by qRT-PCR.
943 Asterisks represent statistical significance (* $p<0.05$, *** $p<0.001$) by two-way ANOVA.
944
945

bioRxiv preprint doi: https://doi.org/10.1101/2022.10.24.513634; this version posted October 25, 2022. The copyright holder for this preprint (which was not certified by peer review) is the author/funder, who has granted bioRxiv a license to display the preprint in perpetuity. It is made available under aCC-BY-NC-ND 4.0 International license.

946 **Table 1: Collaborative Cross mouse lines used in this study.**

CC Line	Legend Symbol	*Oas1b* allele	POWV LB (Fig. 2)		POWV MB5/12 (Fig. 3)	
			% Lethality	MTD	% Lethality	MTD
CC001		Null	83	12.7	-	-
CC003		WSB	-	-	0	N/A
CC004		PWK	-	-	0	N/A
CC006		Null	100	8.8	56	15.9
CC013		Null	100	9.3	-	-
CC015		Null	100	8.3	100	9.3
CC016		Null	100	10.3	-	-
CC019		WSB	-	-	-	-
CC019-*Oas1b*^{del}		Null	78	12.9	38	16.5
CC021		Null	100	9.2	-	-
CC026		Null	100	9.5	-	-
CC027		Null	83	10.8	-	-
CC030		WSB	-	-	0	N/A
CC043		Null	67	13.2	-	-
CC045		Null	0	N/A	22	18.4
CC049		Null	100	10.2	-	-
CC051		Null	100	12.7	-	-
CC057		Null	50	16.5	0	N/A
CC061		Null	100	9.1	-	-
CC062		Null	67	15.2	-	-
CC071		Null	100	8.2	100	9.1

947

948 CC: Collaborative Cross
949 MTD: mean time to death (days)
950 -: not done
951 N/A: not applicable